Four-point functions and kaon decays in a minimal AdS/QCD model

Thomas Hambye,[1,2,*] Babiker Hassanain,[1,†] John March-Russell,[1,‡] and Martin Schvellinger[1,§]

[1]*The Rudolf Peierls Centre for Theoretical Physics, Department of Physics,
University of Oxford, 1 Keble Road, Oxford, OX1 3NP, United Kingdom*

[2]*IFT-UAM/CSIC, Facultad de Ciencias, Universidad Autónoma de Madrid, Cantoblanco, 28049 Madrid, Spain*

We study the predictions of holographic QCD for various observable four-point quark-flavor current-current correlators. The dual 5-dimensional bulk theory we consider is a $SU(3)_L \times SU(3)_R$ Yang-Mills theory in a slice of AdS_5 spacetime with boundaries. Particular UV and IR boundary conditions encode the spontaneous breaking of the dual 4D global chiral symmetry down to the $SU(3)_V$ subgroup. We explain in detail how to calculate the 4D four-point quark-flavor current-current correlators using the 5D holographic theory, including interactions. We use these results to investigate predictions of holographic QCD for the $\Delta I = 1/2$ rule for kaon decays and the B_K parameter. The results agree well in comparison with experimental data, with an accuracy of 25% or better. The holographic theory automatically includes the contributions of the meson resonances to the four-point correlators. The correlators agree well in the low-momentum and high-momentum limit, in comparison with chiral perturbation theory and perturbative QCD results, respectively.

PACS numbers: 11.15.−q, 11.25.Tq, 13.20.Eb, 13.25.Es

I. INTRODUCTION

The success of the perturbative description of QCD allows us to understand the high energy behavior of strong interactions above 1.5 GeV. On the other hand, chiral perturbation theory (χPT) describes well the physics of strong interactions at low energy. In the intermediate region between both regimes, the situation is much less clear since neither of these theories behave perturbatively. One interesting and potentially powerful new idea to gain access to the nonperturbative regime of QCD is holographic QCD, which is based on the gauge/gravity duality [1–4].

There are two kinds of holographic QCD dual models: there are 10D models based on string theory and supergravity [5–23], including studies of deep inelastic scattering [24–28], and in addition, there are phenomenologically inspired 5D holographic dual models [29–35]. In both approaches, the description of confinement and chiral symmetry breaking has been tackled, and masses, decay constants, form factors and other properties of mesons have been calculated, yielding remarkably good agreement with experimental data. All of these estimates are based on two-point current correlators, which do not involve bulk interactions and pertain to the low-lying mesons. Given these initial successes, it is important that these holographic dual models of QCD are tested using processes that go beyond the properties of two-point current correlators, and include interactions in the bulk of the 5D theory. One such test is the computation in the 5D holographic theory of connected 4D four-point flavor current correlators, which can be compared with experiment

and, in certain limits, with the results of chiral perturbation theory and perturbative QCD calculations.

In this paper, we shall focus exclusively on such four-point flavor current correlators. These correlators are crucial to the resolution of a long-standing problem in QCD: the $\Delta I = 1/2$ rule, which we will describe in detail in later sections and briefly here. In short, if one neglects CP-violating effects, there are two independent K^0 decays: $K^0 \to \pi^+ \pi^-$ and $K^0 \to \pi^0 \pi^0$. These two decays are combinations of $\Delta I = 1/2$ and $\Delta I = 3/2$ isospin amplitudes, A_0 and A_2, respectively. Experimentally, $\text{Re}A_0/\text{Re}A_2 = 22.2$, and the largeness of this ratio is the $\Delta I = 1/2$ rule. In the chiral limit, these two amplitudes are generally expressed in terms of the g_8 and g_{27} parameters (see for example [36]), both of which depend on integrals over Euclidean momentum of certain four-current correlators. Our aim in this paper is to apply holographic QCD to calculate these observables.[1]

The 4D theory we are trying to model is QCD with three massless quark flavors, possessing a global $SU(3)_L \times SU(3)_R$ symmetry which is spontaneously broken down to the vector subgroup via the quark condensate.[2] The AdS/CFT correspondence then immediately tells us that the dual 5D theory should be a Yang-Mills theory with the $SU(3)_L \times SU(3)_R$ gauge group, with a bi-fundamental bulk scalar field to provide breaking of this symmetry. The gauge fields in 5D couple to the QCD flavor currents, whereas the bulk scalar couples to the bilinear quark

*thomas.hambye@uam.es
†babiker@thphys.ox.ac.uk
‡jmr@thphys.ox.ac.uk
§martin@thphys.ox.ac.uk

---

[1]In a previous article [37], we briefly presented some of our initial results on this subject. In the present work, we significantly extend and improve upon our earlier study.

[2]Note that for simplicity throughout this paper we work in the chiral limit setting bare quark masses to zero, and ignore the anomalous and therefore explicitly broken $U(1)_{\text{axial}}$ symmetry. We hope to return to these issues in a later publication.

operator. In previous models, the inclusion of a bulk scalar field allowed a comprehensive description of chiral symmetry breaking [29,30,32,33]. However, it is possible to take a limit of this theory where the entire description of chiral symmetry breaking is encoded into the boundary conditions imposed on the gauge fields [30,31] and the holographic theory contains only gauge fields in the bulk. This simplified holographic dual model turns out to be a reasonable approximation [30,31], giving good results at least at the level of the two-point functions. The reason is that the condensate is an infrared (IR) effect, so that its influence can be modeled by an IR boundary condition. The complexity of the calculation of four-point current correlators in AdS/QCD means that this simpler form of holographic QCD, with only gauge fields in the bulk, provides an important starting point that can then be further refined.

Our results are encouraging for AdS/QCD. As we discuss in detail in Secs. V and VI, we find that at leading order in a low-momentum expansion, the behavior of the relevant correlators calculated in holographic QCD agrees with previous calculations using chiral perturbation theory, while at high momentum we obtain the behavior predicted by perturbative QCD. In the intermediate region, the momentum behavior is governed by the exchange of meson resonances, and a significant advantage of the holographic calculation is that it automatically and consistently includes the contribution of the infinite tower of meson resonances to the relevant correlators. Turning to a comparison with the experimental data, the results of a fit of the holographic predictions agree well, with an accuracy of 25% or better, which for quantities as difficult to calculate as the isospin amplitudes $\mathrm{Re}A_0$ and $\mathrm{Re}A_2$, is remarkable. Finally, we hope that the techniques developed here may be useful for more general calculations of n-point global symmetry current correlators in many AdS/CFT holographic dual models.

This paper is organized as follows: In Secs. II and III we introduce the holographic QCD model that we use and present the relevant 5D propagators and interactions. In Sec. IV we discuss the $\Delta I = 1/2$ observables from the viewpoint of QCD, as well as a related but simpler observable $\hat{B}_K$, parametrizing $K^0 - \bar{K}^0$ mixing. We shall also define the nature of the four-current correlators that we calculate using the holographic dual model, and the dependence of the parameters g_8, g_{27}, and $\hat{B}_K$ on these correlators. We also review the χPT predictions for the various observables. In Sec. V we discuss the philosophy of the calculation and present the sum of the 5D Witten diagrams relevant for four-point functions. Section VI contains our numerical results, and our conclusions are given in Sec. VII, where we also briefly address the limitations of the model and possible avenues of improvement. Finally, four appendices contain technical details of the holographic calculation.

Before we start upon our analysis we think it may be useful to offer the readers a ''road map'' to follow the contents of this paper, depending on their particular interests. For readers interested in the AdS/QCD model and calculations of n-point correlators, and, in particular, four-point current correlators, Secs. II, III, and V, supplemented with Appendices A, B, C, and D are recommended. For those interested in the physics of the kaon decays from χPT and perturbative QCD, Sec. IV is relevant. Readers interested in the comparison of the holographic calculation with the experimental results are directed towards Sec. VI.

II. THE 5D HOLOGRAPHIC MODEL

Motivated by the AdS/CFT correspondence, and following on from the work of Refs. [29–33], we consider a 5D bulk theory defined in a constant curvature spacetime with the minimal field content as to describe current-current correlators in QCD. The spacetime metric is that of AdS$_5$ space

$$ds^2 = a^2(z)(\eta_{\mu\nu}dx^\mu dx^\nu - dz^2), \quad (1)$$

where $a(z) = L/z$, L being the curvature scale of the anti-de Sitter space. The 5th-dimensional coordinate z holographically represents the energy scale of the 4D theory. We take z to extend from a UV boundary at $z = L_0$ to an IR boundary at $z = L_1 > L_0$.

We are only interested in spin-1 4D operators such as $\bar{q}_L\gamma^\mu t^a q_L$ and $\bar{q}_R\gamma^\mu t^a q_R$, where q can be u, d, and s quarks. Using the well-known AdS/CFT relation between the dimension of such spin-1 boundary-theory operators Δ and the mass of the bulk vector fields m_5, $(\Delta + 1)(\Delta - 3) = m_5^2$, we find that $\Delta = 3$ gives $m_5 = 0$. We consider the chiral limit of QCD where the quarks are massless, so that global flavor currents are conserved and the boundary symmetry group is a global $SU(3)_L \times SU(3)_R$.

The rules of the holographic correspondence then tell us that the bulk theory is a pure 5D Yang-Mills with *gauge* group $SU(3)_L \times SU(3)_R$. The boundary conditions on the UV brane $z = L_0$ are such that the zero modes of the gauge fields in the μ directions are eliminated, so that no massless 4D gauge symmetry survives. The Lagrangian is given by [29–31]

$$\mathcal{L}_{5D} = \sqrt{g}M_5 \mathrm{Tr}(-\tfrac{1}{4}L_{MN}L^{MN} - \tfrac{1}{4}R_{MN}R^{MN}). \quad (2)$$

The scale M_5 is some yet undetermined mass scale, g is the determinant of the metric, and $M = (\mu, 5)$, where $\mu = 1, \cdots, 4$. The trace Tr is taken over the gauge group indices.

We have $L_M = L_M^a T^a$ and similarly for R_M, where T^a are the Hermitian generators for the Lie Algebra of the $SU(3)_L$ and $SU(3)_R$ groups, satisfying the following commutation relations and normalizations

$$[T^a, T^b] = if^{abc}T^c \quad \text{and} \quad \mathrm{Tr}[T^a T^b] = \delta^{ab}. \quad (3)$$

The f^{abc}'s are real and antisymmetric in this basis. We write the following expressions for the gauge field strengths

$$L_{MN} = \partial_M L_N - \partial_N L_M - i[L_M, L_N], \qquad (4)$$

$$R_{MN} = \partial_M R_N - \partial_N R_M - i[R_M, R_N], \qquad (5)$$

which give us the following relation

$$L_{MN}^a = \partial_M L_N^a - \partial_N L_M^a + f^{abc} L_M^b L_M^c, \qquad (6)$$

and similarly for R_{MN}.

We wish to work with the vector and axial-vector combinations of these gauge fields, so we define

$$V_M = \frac{1}{\sqrt{2}}(L_M + R_M), \qquad (7)$$

$$A_M = \frac{1}{\sqrt{2}}(L_M - R_M). \qquad (8)$$

The reason behind this choice is simple: the spontaneous breaking of chiral symmetry mixes the L_M and R_M gauge fields at the quadratic level. Therefore, the choice of basis as vector and axial-vector rather than left- and right-handed can be viewed as a diagonalization of the equations of motion. Of course, at the cubic and quartic interaction level, there is mixing between V_M and A_M, a fact which is integral to the calculation presented in this article.

We can then express the Lagrangian above entirely in terms of vector and axial-vector fields. To eliminate the mixing between V_μ and V_5 and between A_μ and A_5, we need to include the following R_ξ gauge fixing terms

$$\mathcal{L}_{\mathrm{GF}}^V = -\frac{M_5 a}{2\xi} \mathrm{Tr}\left(\eta^{\mu\nu}\partial_\mu V_\nu - \frac{\xi}{a}\partial_5(aV_5)\right)^2, \quad (9)$$

$$\mathcal{L}_{\mathrm{GF}}^A = -\frac{M_5 a}{2\xi} \mathrm{Tr}\left(\eta^{\mu\nu}\partial_\mu A_\nu - \frac{\xi}{a}\partial_5(aA_5)\right)^2, \quad (10)$$

where ξ is the gauge parameter.

We will go into unitary gauge in what follows, taking the limit $\xi \to \infty$ at the appropriate stages of the calculations. Note that this will have different effects on the vector and axial-vector sectors, due to the different boundary conditions we impose, as explained below. In the next section, we present the full Lagrangian in terms of V_M and A_M, and discuss the IR boundary conditions at $z = L_1$, which correspond to spontaneously breaking the global $SU(3)_L \times SU(3)_R$ symmetry down to its $SU(3)_V$ subgroup.

III. PROPAGATORS AND INTERACTIONS

As we later discuss in detail in Sec. IV, we wish to calculate certain four-point current correlators involving two left-handed and two right-handed currents. We can expand the relevant desired correlator in terms of the vector and axial-vector currents J_V^μ and J_A^μ, so that we can use the bulk Lagrangian in terms of the vector and axial-vector fields.

According to the AdS/CFT correspondence, the boundary values of V_μ and A_μ are classical sources coupling to J_V^μ and J_A^μ, respectively. In order to calculate tree-level n-point functions for the currents, we need to solve the bulk equations of motion for the vector and axial-vector fields, substitute back into the action, and treat this as the generating functional of the boundary theory. One thus has

$$\left\langle e^{\int d^4 x J_V^\mu(x)v_\mu(x)+J_A^\mu(x)a_\mu(x)}\right\rangle = e^{-S_{\mathrm{AdS}}}, \qquad (11)$$

where S_{AdS} is the Euclidean classical bulk action calculated with $V_\mu|_{UV} = v_\mu$ and $A_\mu|_{UV} = a_\mu$. We therefore need the bulk-to-bulk and bulk-to-boundary propagator for each of the gauge fields in the AdS field theory [3,38]. The former allows us to construct the solution to the equations of motion from the interactions in the bulk of the AdS space, and the latter allows the construction of the solution of the equations of motion from the UV boundary value of the field. Green's second theorem gives us a straightforward relation between the two types of propagators.

The procedure of finding the on-shell AdS action subject to certain boundary values of the fields can equivalently be formulated in terms of Witten diagrams, where one uses the vertices of the bulk theory to construct all the allowed Feynman diagrams connecting the boundary operators. The ingredients are the propagators and the vertices, as calculated from the bulk Lagrangian. In this section, we describe how to calculate the propagators. The vertices are simply derived from the full Lagrangian given in Eqs. (12)–(17). We first justify our choices of boundary conditions for the various fields.

Using the variational principle, the bulk equations of motion can be derived, along with the constraints that must be obeyed by any set of consistent boundary conditions. The UV boundary conditions on the bulk-to-bulk propagators can be chosen to be null Dirichlet for both the vector and axial-vector sectors. The IR boundary conditions distinguish the sectors, and allow chiral symmetry breaking (χSB) to be implemented into our model, by imposing null Neumann and null Dirichlet conditions on the vector and axial-vector sectors, respectively. This choice can be understood via an elegant argument: one can consider a bi-fundamental scalar living on the IR brane which acquires a vacuum expectation value. The effect of this on the boundary conditions is simple: it does not affect the vector sector, but changes the boundary conditions on the axial-vector fields from Neumann to mixed. This breaks the chiral symmetry spontaneously, and in theory we have one parameter to play with, analogous to the size of the quark condensate. Now, imagine removing the brane scalar from the theory by allowing its mass to go to infinity. The boundary condition on the axial-vector fields is now found to be a null Dirichlet condition. We also lose the parameter that allows us to tune the size of the symmetry breaking

relative to the scale $1/L_1$, which is set by the IR brane position.

The final requirement is of course to account for the pions, which form a massless pseudoscalar octet. We do this as follows: we impose warped Neumann boundary conditions on the A_5 field on both branes. This guarantees that even after going to unitary gauge in the axial sector, a zero mode remains in A_5 and cannot be gauged away. In the vector sector, we impose Dirichlet conditions on both branes for V_5, so that going into unitary gauge here removes V_5 from the theory.

A. Interaction terms

Here, we display the full boundary Lagrangian and bulk Lagrangian. Note that in the quadratic part, we have taken the limit $\xi \to \infty$ inside the differential operator acting on A_μ and V_μ, but not in the A_5 operator. The quadratic part of the Lagrangian is used to calculate the propagators as shown below. The interaction Lagrangian provides the vertices needed to construct the Witten diagrams relevant for the calculation of any given n-point boundary current correlator. The full 5D Lagrangian can be written as a sum of the following terms, where the trace over the gauge indices is implicit

$$\mathcal{L}_{\text{boundary}} = \left[\frac{M_5 L}{2z} \eta^{\mu\nu} (V_\nu \partial_5 V_\mu + A_\nu \partial_5 A_\mu \right.$$
$$\left. - 2A_\mu \partial_\nu A_5) \right]_{L_0}^{L_1}, \qquad (12)$$

$$\mathcal{L}_{\text{quadratic}} = \frac{M_5 L}{2z} \left[V_\mu \left(\partial^2 \eta^{\mu\nu} - z\partial_z \left(\frac{1}{z}\partial_z \right) \eta^{\mu\nu} - \partial^\mu \partial^\nu \right) \right.$$
$$\times V_\nu A_\mu \left(\partial^2 \eta^{\mu\nu} - z\partial_z \left(\frac{1}{z}\partial_z \right) \eta^{\mu\nu} - \partial^\mu \partial^\nu \right) A_\nu$$
$$\left. + A_5(-\partial^2)A_5 + \xi A_5 \partial_z \left(z\partial \left(\frac{1}{z}A_5 \right) \right) \right], \qquad (13)$$

$$\mathcal{L}_{VAA_5, VA_5A_5} = -i\frac{M_5 L}{\sqrt{2}z} \eta^{\mu\nu} (\partial_5 V_\mu[A_5, A_\nu]$$
$$+ \partial_5 A_\mu[A_5, V_\nu] + \partial_\mu A_5[V_\nu, A_5]), \qquad (14)$$

$$\mathcal{L}_{\text{3-vector}} = i\frac{M_5 L}{\sqrt{2}z} \eta^{\mu\rho} \eta^{\nu\sigma} (\partial_\mu V_\nu[A_\rho, A_\sigma]$$
$$+ \partial_\mu A_\nu[V_\rho, A_\sigma] + \partial_\mu A_\nu[A_\rho, V_\sigma]$$
$$+ \partial_\mu V_\nu[V_\rho, V_\sigma]), \qquad (15)$$

$$\mathcal{L}_{\text{4-vector}} = \frac{M_5 L}{4z} \eta^{\mu\rho} \eta^{\nu\sigma} (V_\mu V_\nu[V_\rho, V_\sigma]$$
$$+ A_\mu A_\nu[A_\rho, A_\sigma] + 4V_\mu V_\nu A_\rho A_\sigma$$
$$- 2V_\mu V_\nu A_\sigma A_\rho + 2V_\mu A_\nu V_\rho A_\sigma$$
$$- 2V_\mu A_\nu A_\sigma V_\rho - A_\mu V_\rho A_\nu V_\sigma$$
$$- V_\mu A_\rho V_\nu A_\sigma), \qquad (16)$$

$$\mathcal{L}_{VVA_5A_5, AAA_5A_5} = -\frac{M_5 L}{2z} \eta^{\mu\nu} (V_\mu A_5[V_\nu, A_5]$$
$$+ A_\mu A_5[A_\nu, A_5]). \qquad (17)$$

Examining the boundary Lagrangian in Eq. (12), one immediately sees the familiar terms that are bilinear in V_μ and A_μ. These are responsible for the emission of vector and axial-vector resonances by the boundary-theory current. The unusual term here is the mixing term between A_μ and A_5, which says that a boundary axial current can emit an A_5 particle. This term survives the application of the boundary conditions, and is in fact of paramount importance in the satisfaction of the Ward identities. This can be seen from a calculation of the axial current two-point function as described in Appendix C. The Ward identity requires this correlator to be transverse, but this is only achieved by the AdS/CFT computation if one takes into account a diagram where the A_5 field is emitted by one current and absorbed by the other.

Finally, it is clear that the inclusion of the higher dimensional operators $\text{Tr}(L_{MN}^3 + R_{MN}^3)$ and $\text{Tr}(L_{MN}^4 + R_{MN}^4)$ in the Lagrangian of Eq. (2) results in other three-boson and four-boson vertices. However, one can show that they are subleading in the large $M_5 L$ or, equivalently, the large-N_c limit, once one recognizes that $M_5 L$ goes like N_c parametrically, as in Refs. [29,30]. The argument goes as follows: the Lagrangian in five dimensions has the schematic form given by

$$\mathcal{L}_{\text{5D}} = M_5 L \left[\frac{\sqrt{g}}{L} \text{Tr}(F^2) + c_1 \frac{\sqrt{g}}{L} \frac{\text{Tr}(F^3)}{M_5^2} \right.$$
$$\left. + c_2 \frac{\sqrt{g}}{L} \frac{\text{Tr}(F^4)}{M_5^4} + \cdots \right], \qquad (18)$$

where $\text{Tr}(F^2)$ represents the leading terms of the gauge field theory as written in Eq. (2), i.e. $\text{Tr}(L_{MN}L^{MN} + R_{MN}R^{MN})$, and the other terms signify higher dimensional operators, an example being $\text{Tr}(g^{MS}g^{NQ}g^{PR}L_{MN} \times L_{SP}L_{QR} + L \to R)$. Now, when we write this in terms of the fields A_μ, V_μ and A_5, V_5, we must remember that each factor of field strength F comes in with a factor of g^{MN}. A factor of g^{MN} brings with it a factor z^2/L^2. Recall also that $\sqrt{g} = (L/z)^5$. Thus, we can schematically write:

$$L_{5D} = M_5 L \left[\frac{1}{z} \, \mathrm{Tr}(F_{dd} F_{dd}) + c_1 \frac{z}{(M_5 L)^2} \, \mathrm{Tr}(F_{dd} F_{dd} F_{dd}) \right.$$
$$\left. + c_2 \frac{z^3}{(M_5 L)^4} \, \mathrm{Tr}(F_{dd} F_{dd} F_{dd} F_{dd}) + \cdots \right], \quad (19)$$

where F_{dd} simply means L_{MN}, R_{MN}, i.e. the field strength with lower Lorentz indices. More generally, a gauge invariant operator with n factors of F will have a coefficient that goes like $c_{n-2} z^{2n-5}/(M_5 L)^{2(n-2)}$, where all the c factors are of order one. This means that, in the large-N_c limit, the contribution from these operators is subleading to that from the term $\mathrm{Tr}(L_{MN} L^{MN} + R_{MN} R^{MN})$, as claimed.

B. $SU(3)_V$ sector propagators

The vector *bulk-to-bulk* propagator has a transverse and longitudinal part, because we are working in the gauge $V_5 = 0$ (unitary gauge). The value of V_μ at the UV boundary is the classical source to which the 4D current J_V^μ couples. On the IR boundary, we impose a Neumann condition on the vector field. We write (following [39])

$$\langle V^\mu V^\nu \rangle = -i G_p^V(z, z') \left(\eta^{\mu\nu} - \frac{p^\mu p^\nu}{p^2} \right) - i G_0^V(z, z')$$
$$\times \left(\frac{p^\mu p^\nu}{p^2} \right). \quad (20)$$

Note that we are working in Lorentz indices, so we lower and raise these indices with the 4D Poincaré metric $\eta^{\mu\nu}$. In Fourier space in the x^μ directions, but position space for the 5th direction, the propagators solve the equation

$$\left(\partial_z^2 - \frac{1}{z} \partial_z + p^2 \right) G_p^V(z, z') = \frac{z}{M_5 L} \delta(z - z'). \quad (21)$$

In addition, $G_0^V(z, z')$ solves the same equation with p set to zero. The boundary conditions on $G_p^V(z, z')$ are Dirichlet on the UV brane and Neumann on the IR brane, so that

$$G_p^V(z, z')|_{z=L_0} = 0, \quad (22)$$

$$\partial_z G_p^V(z, z')|_{z=L_1} = 0. \quad (23)$$

From Green's second theorem, the *bulk-to-boundary* propagator is defined by the following limit

$$\langle V^\mu V^\nu \rangle|_{\partial \mathrm{ADS}}(z') = -\frac{M_5 L}{z} \partial_z \langle V^\mu V^\nu \rangle|_{z=L_0}, \quad (24)$$

where

$$\langle V^\mu V^\nu \rangle|_{\partial \mathrm{ADS}}(z') = -i K_p^V(z') \left(\eta^{\mu\nu} - \frac{p^\mu p^\nu}{p^2} \right)$$
$$- i K_0^V(z') \left(\frac{p^\mu p^\nu}{p^2} \right). \quad (25)$$

The solutions are given by [29–31]

$$G_p^V(z, z')_{z<z'} = \frac{\pi z z'}{2 M_5 L (AD - BC)} [A \mathcal{J}_1(pz) + B \mathcal{Y}_1(pz)]$$
$$\times [C \mathcal{J}_1(pz') + D \mathcal{Y}_1(pz')], \quad (26)$$

$$G_p^V(z, z')_{z>z'} = \frac{\pi z z'}{2 M_5 L (AD - BC)} [A \mathcal{J}_1(pz') + B \mathcal{Y}_1(pz')]$$
$$\times [C \mathcal{J}_1(pz) + D \mathcal{Y}_1(pz)], \quad (27)$$

where

$$A = -\mathcal{Y}_1(pL_0), \qquad C = -\mathcal{Y}_0(pL_1),$$
$$B = \mathcal{J}_1(pL_0), \qquad D = \mathcal{J}_0(pL_1), \quad (28)$$

and

$$G_0^V(z, z')_{z<z'} = -\frac{1}{2 M_5 L}(z^2 - L_0^2), \quad (29)$$

$$G_0^V(z, z')_{z>z'} = -\frac{1}{2 M_5 L}(z'^2 - L_0^2). \quad (30)$$

Here $\mathcal{J}$ and $\mathcal{Y}$ are Bessel functions of the first and second kind in the conventions of Ref. [40]. From these bulk-to-bulk propagators, we find that the bulk-to-boundary propagators are given by

$$K_p^V(z') = -\frac{z'}{L_0} \frac{[C \mathcal{J}_1(pz') + D \mathcal{Y}_1(pz')]}{[AD - BC]}, \quad (31)$$

$$K_0^V(z') = 1. \quad (32)$$

Note that in calculating the bulk-to-boundary propagator, we use the bulk-to-bulk propagator for $z < z'$, so that

$$K_p^V(z') = -\frac{M_5 L}{z} \partial_z G_p^V(z, z')_{z<z'}|_{z=L_0}, \quad (33)$$

$$K_0^V(z') = -\frac{M_5 L}{z} \partial_z G_0^V(z, z')_{z<z'}|_{z=L_0}. \quad (34)$$

C. $SU(3)_A$ sector propagators

We here list the propagators for A_μ and A_5. As explained above, the IR boundary conditions in this sector are chosen so that the $SU(3)_L \times SU(3)_R$ global chiral symmetry is spontaneously broken:

$$G_p^A(z, z')|_{z=L_0} = 0, \quad (35)$$

$$G_p^A(z, z')|_{z=L_1} = 0. \quad (36)$$

Similar to the $SU(3)_V$ sector we define

$$\langle A^\mu A^\nu \rangle = -i G_p^A(z, z') \left(\eta^{\mu\nu} - \frac{p^\mu p^\nu}{p^2} \right)$$
$$- i G_0^A(z, z') \left(\frac{p^\mu p^\nu}{p^2} \right). \quad (37)$$

The equation to be solved is the same as in the $SU(3)_V$ sector. The results are [29–31]

$$G_p^A(z, z')_{z<z'} = \frac{\pi z z'}{2M_5 L(A\bar{D} - B\bar{C})}[A\mathcal{J}_1(pz) + B\mathcal{Y}_1(pz)]$$
$$\times [\bar{C}\mathcal{J}_1(pz') + \bar{D}\mathcal{Y}_1(pz')], \qquad (38)$$

$$G_p^A(z, z')_{z>z'} = \frac{\pi z z'}{2M_5 L(A\bar{D} - B\bar{C})}[A\mathcal{J}_1(pz') + B\mathcal{Y}_1(pz')]$$
$$\times [\bar{C}\mathcal{J}_1(pz) + \bar{D}\mathcal{Y}_1(pz)], \qquad (39)$$

where A and B are as for the $SU(3)_V$ sector, and

$$\bar{C} = -\mathcal{Y}_1(pL_1), \qquad \bar{D} = \mathcal{J}_1(pL_1). \qquad (40)$$

This gives us

$$G_0^A(z, z')_{z<z'} = -\frac{1}{2M_5 L}(z^2 - L_0^2)\frac{z'^2 - L_1^2}{L_0^2 - L_1^2}, \qquad (41)$$

$$G_0^A(z, z')_{z>z'} = -\frac{1}{2M_5 L}(z'^2 - L_0^2)\frac{z^2 - L_1^2}{L_0^2 - L_1^2}. \qquad (42)$$

From these propagators, we obtain the bulk-to-boundary propagators as for the $SU(3)_V$ case, to find that

$$K_p^A(z') = -\frac{z'}{L_0}\frac{[\bar{C}\mathcal{J}_1(pz') + \bar{D}\mathcal{Y}_1(pz')]}{[A\bar{D} - B\bar{C}]}, \qquad (43)$$

$$K_0^A(z') = \frac{z'^2 - L_1^2}{L_0^2 - L_1^2}. \qquad (44)$$

We also note that the current-current correlator as $p \to 0$ is now given by (see Appendix C)

$$\Pi_A(p^2)|_{p=0} = F_\pi^2 = \frac{2M_5 L}{L_1^2 - L_0^2}. \qquad (45)$$

This is a direct consequence of the IR boundary condition. The A_5 propagator in this gauge is simply given by

$$\langle A_5 A_5 \rangle = -iG_p^5(z, z'), \qquad (46)$$

where $G_p^5(z, z')$ is the limit as $\xi \to \infty$ of the solution to the equation

$$\left(\xi\partial_z^2 - \xi\frac{1}{z}\partial_z + \xi\frac{1}{z^2} + p^2\right)G_p^5(z, z') = -\frac{z}{M_5 L}\delta(z - z'), \qquad (47)$$

with the boundary conditions

$$\partial_z(aG_p^5(z, z'))|_{z=L_0} = 0, \qquad (48)$$

$$\partial_z(aG_p^5(z, z'))|_{z=L_1} = 0, \qquad (49)$$

giving[3]

_____

[3]Note the factor 2 difference between the A_5 propagator here and the (incorrect) one used in our previous paper [37].

$$G_p^5(z, z') = \frac{-2zz'}{M_5 L[L_1^2 - L_0^2]}\left(\frac{1}{p^2}\right). \qquad (50)$$

IV. FOUR-POINT OBSERVABLES

A. The $\Delta I = 1/2$ rule

Neglecting CP violation effects, there are two independent $K \to \pi\pi$ decay amplitudes, $K^0 \to \pi^+\pi^-$ and $K^0 \to \pi^0\pi^0$. These amplitudes can be written in terms of the $\Delta I = 1/2$ amplitude A_0 and the $\Delta I = 3/2$ amplitude A_2 as

$$A(K^0 \to \pi^+\pi^-) = A_0 e^{i\delta^0} + \sqrt{1/2}A_2 e^{i\delta_2}, \qquad (51)$$

$$A(K^0 \to \pi^0\pi^0) = A_0 e^{i\delta^0} - \sqrt{2}A_2 e^{i\delta_2}. \qquad (52)$$

The measured values of these amplitudes are

$$\text{Re}\,A_0 = 2.72 \times 10^{-4} \text{ MeV},$$
$$\text{Re}A_2 = 1.22 \times 10^{-5} \text{ MeV}, \qquad (53)$$

which gives

$$\frac{1}{\omega} \equiv \frac{\text{Re}A_0}{\text{Re}A_2} \equiv \frac{\text{Re}(K \to (\pi\pi)_{I=0})}{\text{Re}(K \to (\pi\pi)_{I=2})} = 22.2. \qquad (54)$$

The large value of $\text{Re}A_0/\text{Re}A_2$ is the so-called $\Delta I = 1/2$ rule.

In the following, we use holographic QCD to calculate $\text{Re}A_0$ and $\text{Re}A_2$ in the chiral limit. In this limit, at order p^2 in the chiral counting, all the $\Delta S = 1$ transitions can be obtained from the standard $\Delta S = 1$ effective Lagrangian, involving the usual g_8 and g_{27} coupling constants (neglecting the small electromagnetic contribution, see for example [36,41])

$$\mathcal{L}_{\text{eff}}^{\Delta S=1} = -\frac{G_\text{F}}{\sqrt{2}}V_{ud}V_{us}^*[g_8\mathcal{L}_8 + g_{27}\mathcal{L}_{27}], \qquad (55)$$

where

$$\mathcal{L}_8 = \sum_{i=1,2,3}(\mathcal{L}_\mu)_{2i}(\mathcal{L}^\mu)_{i3} \quad \text{and}$$
$$\mathcal{L}_{27} = \frac{2}{3}(\mathcal{L}_\mu)_{21}(\mathcal{L}^\mu)_{13} + (\mathcal{L}_\mu)_{23}(\mathcal{L}^\mu)_{11}, \qquad (56)$$

with

$$\mathcal{L}_\mu = -iF_\pi^2 U(x)^\dagger D_\mu U(x), \qquad (57)$$

and $V_{ud} = 0.974$, $V_{us} = 0.224$. The pion decay constant F_π is taken in the chiral limit, where the masses of the u, d, and s quarks are neglected ($F_\pi \simeq 87$ MeV). The matrix field U collects the Goldstone bosons of the spontaneously broken chiral symmetry of the QCD Lagrangian with three massless flavors, and $D_\mu U$ denotes the covariant derivative: $D_\mu U = \partial_\mu U - ir_\mu U + iUl_\mu$, in the presence of external chiral sources l_μ and r_μ of left- and right-handed currents. The parameters g_8 and g_{27} encode the dynamics

of the integrated-out degrees of freedom in the chiral limit. These include the heavy quark flavors as well as the light hadronic flavor states. Notice that the octet term proportional to g_8 induces pure $\Delta I = 1/2$ transitions, while the term proportional to g_{27} induces both $\Delta I = 1/2$ and $\Delta I = 3/2$ transitions:

$$A_0 = -\frac{G_F}{\sqrt{2}} V_{ud} V_{us}^* \sqrt{2} F_\pi \left(g_8 + \frac{1}{9} g_{27}\right)(M_K^2 - m_\pi^2), \quad (58)$$

$$A_2 = -\frac{G_F}{\sqrt{2}} V_{ud} V_{us}^* 2 F_\pi \frac{5}{9} g_{27}(M_K^2 - m_\pi^2), \quad (59)$$

where M_K and m_π are the masses of the kaon and the pion, respectively, and G_F is the Fermi four-point interaction parameter.

To calculate g_8 and g_{27}, we separate the long and short distance contributions as usual and perform an operator product expansion (OPE), obtaining the effective Hamiltonian for $|\Delta S| = 1$ transitions [42–44],

$$\mathcal{H}_{\text{eff}}^{\Delta S=1} = \frac{G_F}{\sqrt{2}} \xi_u \sum_{i=1}^{8} c_i(\mu) Q_i(\mu) \quad (60)$$

$$(\mu < m_c = \text{charm quark mass}),$$

$$c_i(\mu) = z_i(\mu) + \tau y_i(\mu), \quad \tau = -\xi_t/\xi_u, \quad \xi_q = V_{qs}^* V_{qd}. \quad (61)$$

The arbitrary renormalizsation scale μ separates short- and long-distance contributions to the decay amplitudes. The Wilson coefficient functions $c_i(\mu)$ contain all the information on heavy-mass scales. For *CP* conserving processes, the contribution involving the Cabibbo-Kobayashi-Maskawa (CKM) elements of the top quark, encoded in $y_i(\mu)$, is negligible and only the $z_i(\mu)$ are numerically relevant. The coefficient functions can be calculated for a scale $\mu \gtrsim 1$ GeV using perturbative renormalization group techniques. They were computed in an extensive next-to-leading logarithm analysis by two groups [45,46]. After Fierz reordering, the local four-quark operators $Q_i(\mu)$ can be written in terms of color singlet quark bilinears

$$Q_1 = 4\bar{s}_L \gamma^\mu d_L \bar{u}_L \gamma_\mu u_L, \quad Q_2 = 4\bar{s}_L \gamma^\mu u_L \bar{u}_L \gamma_\mu d_L,$$

$$Q_3 = 4\sum_q \bar{s}_L \gamma^\mu d_L \bar{q}_L \gamma_\mu q_L, \quad Q_4 = 4\sum_q \bar{s}_L \gamma^\mu q_L \bar{q}_L \gamma_\mu d_L,$$

$$Q_5 = 4\sum_q \bar{s}_L \gamma^\mu d_L \bar{q}_R \gamma_\mu q_R, \quad Q_6 = -8\sum_q \bar{s}_L q_R \bar{q}_R d_L,$$

$$Q_7 = 4\sum_q \frac{3}{2} e_q \bar{s}_L \gamma^\mu d_L \bar{q}_R \gamma_\mu q_R,$$

$$Q_8 = -8\sum_q \frac{3}{2} e_q \bar{s}_L q_R \bar{q}_R d_L, \quad (62)$$

where the sum goes over the light flavors ($q = u, d, s$) and

$$q_{R,L} = \frac{1}{2}(1 \pm \gamma_5)q, \qquad e_q = (2/3, -1/3, -1/3). \quad (63)$$

The operators $Q_3, \ldots, Q_6$ arise from QCD penguin diagrams involving a virtual W and a c or t quark, with gluons connecting the virtual heavy quark to light quarks. They transform as $(8_L, 1_R)$ under $SU(3)_L \times SU(3)_R$ and solely contribute to $\Delta I = 1/2$ transitions. It is important to note that they are present only below the charm threshold, i.e. for $\mu < m_c$. Similarly the Wilson coefficients $z_{7,8}$ of the electroweak penguin operators $Q_{7,8}$ are nonzero only for $\mu < m_c$. Thus, in the following, only Q_1 and Q_2 will be considered as we will always work in the regime $\mu \gtrsim m_c$. Long-distance contributions to the amplitudes A_I are contained in the hadronic matrix elements of the four-quark operators,

$$\langle Q_i(\mu)\rangle_I \equiv \langle \pi\pi, I|Q_i(\mu)|K^0\rangle. \quad (64)$$

In the strict large-N_c limit, i.e. considering only the W exchange diagram with $z_2 = 1$ we get $g_8 = g_{27} = 3/5$, while experimentally, from Eqs. (53), (58), and (59), leads to both an enhancement of the $I = 0$ and a suppression of the $I = 2$ final state. The *octet enhancement* [42] in the (Q_1, Q_2) sector is dominated by the increase of z_2 when μ evolves from M_W down to $\mu \simeq 1$ GeV, whereas the suppression of the $\Delta I = 3/2$ transition results from a partial cancellation between the contributions from the Q_1 and Q_2 operators. Taking into account the running of z_1 and z_2 between M_W and $\mu \simeq m_c = 1300$ MeV, which gives $z_1 \simeq -0.5$, $z_2 \simeq 1.3$, and still considering the matrix elements in the large-N_c limit, i.e. considering only the factorizable contribution, one gets $g_8 \simeq 1$ and $g_{27} \simeq 0.5$. This gives values closer to the experimental ones but a factor 5 (3/5) is still missing for g_8 (g_{27}). Thus, perturbative QCD effects are far from sufficient to describe the $\Delta I = 1/2$ rule and QCD dynamics at low energies must be addressed beyond the leading N_c limit, that is to say, at the level of the nonfactorizable contribution [36,47–50].

Further progress was made when, in addition to the $O(p^2)$ weak $\Delta S = 1$ Lagrangian of Eq. (55), the $O(p^4)$ $\Delta S = 1$ Lagrangian was also considered. A full fit of all the weak Lagrangian constants was then carried out, taking into account not only the experimental $K \to \pi\pi$ amplitudes but also the experimental $K \to \pi\pi\pi$ amplitudes. It was found that the $O(p^2)$ contribution is expected to account for $g_8 = 3.3$ and $g_{27} = 0.23$. The rest of the experimental amplitudes are expected to be explained by the $O(p^4)$ $\Delta S = 1$ Lagrangian. Numerically, this $O(p^4)$ higher-order (HO) contribution is equivalent to adding by hand a contribution of $+1.8$ and $+0.06$ to g_8 and g_{27}, respectively. In the following, we will only calculate the $O(p^2)$ Lagrangian constants g_8 and g_{27}, which should account for about two thirds of ReA_0 and three quarters of ReA_2. Therefore, for comparison with experiment, there are two equivalent possibilities: we either compare the values of $g_{8,27}$ we obtain from Eqs. (69) and (70) with the values 3.3 and 0.23 above, or, adding the $O(p^4)$ con-

tribution by hand, we compare the values we get for

$$g_8^{\text{TOT}} = g_8 + g_8^{\text{HO}}, \qquad (65)$$

$$g_{27}^{\text{TOT}} = g_{27} + g_{27}^{\text{HO}}, \qquad (66)$$

with the values 5.1 and 0.29, with $g_8^{\text{HO}} = 1.8$ and $g_{27}^{\text{HO}} = 0.06$.

To calculate the nonfactorizable contribution to g_8 and g_{27}, one can make use of the chiral symmetry properties of the $\Delta S = 1$ effective Lagrangian of Eq. (55). Instead of calculating the $K \to \pi\pi$ amplitudes explicitly, it is much simpler to calculate them taking $U = 1$ in Eq. (55), i.e. considering the processes with no external pseudoscalar and only two external sources coming from the covariant derivatives of U. For reasons explained in Ref. [36] it is convenient to consider the processes with two external right-handed sources (for instance for $\mathcal{L}_8$ we consider $\mathcal{L}_8 \ni \sum_{i=1,2,3} F_\pi^4 (r_\mu)_{2i} (r^\mu)_{i3}$). The nonfactorizable contribution to this process of four-quark operators is then given by Green's functions involving, on the one hand, the two left-handed currents of the four-quark operator inducing this process, and, on the other hand, the two right-handed currents coupling to the right-handed sources. More precisely, including the leading N_c nonfactorizable contribution from Q_1 and Q_2, the parameters g_8 and g_{27} are given by the Q^2 integrals (with p the Minkowski momentum flowing between the two left-handed currents) of the two Green's functions [36,51]:

$$W_{LRLR}^{\mu\alpha\nu\beta}(p) = \lim_{l\to 0} i^3 \int d^4x d^4y d^4z e^{ipx+il(y-z)}$$
$$\times \langle 0|T\{L_{\bar{s}d}^\mu(x) R_{\bar{d}s}^\alpha(y) L_{\bar{s}d}^\nu(0) R_{\bar{d}s}^\beta(z)\}|0\rangle|_{\text{conn}}, \qquad (67)$$

$$W_{LLRR}^{\mu\nu\alpha\beta}(p) = \lim_{l\to 0} i^3 \int d^4x d^4y d^4z e^{ipx+il(y-z)}$$
$$\times \langle 0|T\{L_{\bar{s}u}^\mu(x) L_{\bar{u}d}^\nu(0) R_{\bar{d}u}^\alpha(y) R_{\bar{u}s}^\beta(z)\}|0\rangle|_{\text{conn}}, \qquad (68)$$

with

$$g_8(\mu) = z_1(\mu)\left(-1 + \frac{3}{5}g_{\Delta S=2}(\mu)\right)$$
$$+ z_2(\mu)\left(1 - \frac{2}{5}g_{\Delta S=2}(\mu)\right.$$
$$\left.- \int_0^{\mu^2} dQ^2 \frac{W_{LLRR}(Q^2)}{4\pi^2 F_\pi^2}\right), \qquad (69)$$

$$g_{27}(\mu) = (z_1(\mu) + z_2(\mu))\frac{3}{5}g_{\Delta S=2}(\mu), \qquad (70)$$

and

$$g_{\Delta S=2}(\mu) = 1 - \frac{1}{32\pi^2 F_\pi^2}\int_0^{\mu^2} dQ^2 W_{LRLR}(Q^2), \qquad (71)$$

while

$$W_{LRLR}(Q^2) = -\frac{4}{3}\frac{Q^2}{F_\pi^2}\eta_{\alpha\beta}\eta_{\mu\nu}\int \frac{d\Omega_p}{4\pi} W_{LRLR}^{\mu\alpha\nu\beta}(p), \qquad (72)$$

$$W_{LLRR}(Q^2) = -\frac{1}{3}\frac{Q^2}{F_\pi^2}\eta_{\alpha\beta}\eta_{\mu\nu}\int \frac{d\Omega_p}{4\pi} W_{LLRR}^{\mu\nu\alpha\beta}(p). \qquad (73)$$

Notice that we use the notation Q^2 for the Euclidean momentum (i.e. $Q^2 = -p^2$).

From the above equations we see that the factorizable contributions to g_8 and g_{27} are

$$g_8^F(\mu) = -\frac{2}{5}z_1(\mu) + \frac{3}{5}z_2(\mu), \qquad (74)$$

$$g_{27}^F(\mu) = \frac{3}{5}(z_1(\mu) + z_2(\mu)). \qquad (75)$$

The remaining nonfactorizable parts of Eqs. (69)–(71) are the subject of the calculations of this paper.

In the above, we only consider, as necessary, the connected parts of the four-point functions. The currents are defined by $R_{\bar{q}_1 q_2}^\mu = \bar{q}_1 \gamma^\mu \frac{(1+\gamma_5)}{2} q_2$, $L_{\bar{q}_1 q_2}^\mu = \bar{q}_1 \gamma^\mu \frac{(1-\gamma_5)}{2} q_2$, and the subscript of $g_{\Delta S=2}$ comes from the fact that this quantity also determines the $\Delta S = 2$ transitions (see below).[4]

In order to calculate the integrals of Eqs. (69)–(71), the Q^2 dependence of W_{LLRR} and W_{LRLR} must be determined. However, this dependence is known only in the asymptotic regimes $Q^2 \to 0$ and $Q^2 \to \infty$. In the limit when $Q^2 \to 0$, from χPT [36,51,52], and after a long calculation, one gets

$$W_{LRLR}(Q^2) = 6 - 24(2l_1 + 5l_2 + l_3 + l_9)\frac{Q^2}{F_\pi^2} + \dots, \qquad (76)$$

while for the other correlator only one group has calculated the χPT result [36],

$$W_{LLRR}(Q^2) = -\frac{3}{8} + \left(-\frac{15}{2}l_3 + \frac{3}{2}l_9\right)\frac{Q^2}{F_\pi^2} + \dots \qquad (77)$$

In these expressions the l_i are the standard renormalized $O(p^4)$ chiral Lagrangian coefficients, usually denoted by L_i.

In the limit $Q^2 \to \infty$, and using Shifman-Vainshtein-Zakharov (SVZ) OPE techniques [43], one obtains [36,51]

$$\lim_{Q^2\to\infty} W_{LRLR}(Q^2) = +24\pi^2 \frac{\alpha_s}{\pi}\frac{F_\pi^2}{Q^2}, \qquad (78)$$

---

[4]Notice that Eq. (72) has been modified by a normalization factor 4, of which we were not aware in our previous paper [37]. This normalization is correct when one sums over all possible planar flavor contractions, as we do here.

$$\lim_{Q^2 \to \infty} W_{LLRR}(Q^2) = +\frac{1}{3}\pi^2 \frac{\alpha_s}{\pi} \frac{F_\pi^2}{Q^2} - \frac{16}{3}\pi^2 \frac{\alpha_s}{\pi} \frac{\langle\bar{\psi}\psi\rangle^2 l_5}{F_\pi^4 Q^2},$$

(79)

where α_s is the strong coupling constant, $\langle\bar{\psi}\psi\rangle$ is the quark condensate, and l_5 is one of the $O(p^4)$ chiral Lagrangian coefficients. Note that in Eq. (79) the term depending on $\langle\bar{\psi}\psi\rangle$ is numerically dominant. Using 4D large-N_c diagrammatics, one can see that W_{LRLR} and W_{LLRR} are given by a sum of simple to triple poles in Q^2 multiplied by polynomials in Q^2. Combining this constraint with Eqs. (76)–(79), we then get the most general form for the Green's functions [36,51]

$$W_{LRLR} = \sum_{i=1}^{\infty}\left(\frac{\alpha_i}{(Q^2+M_i^2)} + \frac{\beta_i}{(Q^2+M_i^2)^2} + \frac{\gamma_i}{(Q^2+M_i^2)^3}\right),$$

(80)

$$W_{LLRR} = \sum_{i=1}^{\infty}\left(\frac{\alpha_i'}{(Q^2+M_i^2)} + \frac{\beta_i'}{(Q^2+M_i^2)^2} + \frac{\gamma_i'}{(Q^2+M_i^2)^3}\right),$$

(81)

where the M_i's are the masses of the resonances and α_i, β_i, γ_i, and α_i', β_i', γ_i' are constants.

Quite a few calculations have been proposed in the $1/N_c$ expansion to estimate the Q^2 integrals [36,47–49]. They all found a large enhancement of ReA_0 together with a decrease of ReA_2, so that the bulk of the $\Delta I = 1/2$ rule can be explained. In those references, the size of the enhancement is determined essentially by two distinct factors. The first is the χPT behavior at low scale, as determined by the chiral Lagrangian parameters, and the second is the size of the hadronic scales, namely, the masses of the hadronic resonances, which will modify and terminate this behavior at some higher scale. In particular, see Ref. [36], which explains in detail why the interplay of the relevant hadronic scales—the small chiral constants F_π and $\langle\bar{\psi}\psi\rangle$ on the factorizable side and larger resonance masses on the nonfactorizable side—means that such a large nonfactorizable contribution must be present. However, the effect of the resonances was not calculated explicitly in Refs. [36,47–49], but introduced in an indirect way. In [47,48] only χPT results (Eqs. (76) and (77)) were considered, with a cutoff put by hand at the mass of the resonances. The work of [36] used the form of Eqs. (80) and (81) to interpolate between Eqs. (76)–(79) with a minimum number of resonances, while [49] employed Nambu-Jona-Lasinio models. The implicit assumption of these procedures is that the contribution to W_{LRLR} and W_{LLRR} from the intermediate momentum region (0.5–2 GeV^2) can be obtained via a gentle interpolation (i.e. without "bumps") between the chiral behavior and the OPE behavior. In any case, it is clear that a method incorporating resonances explicitly would be highly preferable. This is precisely where the power of holographic QCD lies, at least for these observables, since

it is a method where the effect of the entire tower of resonances for each channel can, in principle, be calculated.

B. The B_K parameter

From the Green's function W_{LRLR}, there is another observable whose nonfactorizable contribution can be calculated in the chiral limit and at leading N_c order, and which can be used as a test of the holographic method described below. This is the $\hat{B}_K$ observable, parametrizing $K^0 - \bar{K}^0$ mixing. At the quark level, K^0 and $\bar{K}^0$ mix due to a box one-loop diagram where the K^0 transforms itself into a $\bar{K}^0$ through a pair of W bosons. This diagram leads to the following effective Hamiltonian [53]:

$$\mathcal{H}_{\text{eff}}^{\Delta S=2} = \frac{G_F^2 M_W^2}{4\pi^2}[\lambda_c^2 F_1 + \lambda_t^2 F_2 + 2\lambda_c\lambda_t F_3]C_{\Delta S=2}(\mu)Q_{\Delta S=2}(x),$$

(82)

with

$$Q_{\Delta S=2}(x) \equiv (\bar{s}_L(x)\gamma^\mu d_L(x))(\bar{s}_L(x)\gamma_\mu d_L(x)),$$

(83)

and $C_{\Delta S=2}$ is the Wilson coefficient. From this effective Hamiltonian, defining

$$\langle\bar{K}^0|Q_{\Delta S=2}(0)|K^0\rangle \equiv \tfrac{4}{3}f_K^2 M_K^2 B_K(\mu),$$

(84)

the parameter $\hat{B}_K$ is defined as

$$\hat{B}_K \equiv C_{\Delta S=2}(\mu)B_K(\mu).$$

(85)

The large-N_c limit (i.e. the factorizable contribution) gives $B_K = 3/4$.

In the chiral limit and at leading N_c order, it turns out that the nonfactorizable contribution is determined by the same integral of W_{LRLR} as the one found in parts of g_8 and in g_{27}, Eqs. (69)–(71). This gives

$$B_K(\mu) = \tfrac{3}{4}g_{\Delta S=2}(\mu).$$

(86)

These relations come from a dynamical symmetry [54] relating part of the matrix elements of Q_1 and Q_2 with those of $Q_{\Delta S=2}$.

Unfortunately, there is no precise experimental determination of the $\hat{B}_K$ parameter. Thus, for our purposes, we will take $\hat{B}_K = 0.36 \pm 0.15$ as a reference value, as obtained in the chiral limit in Refs. [36,51,55]. Similar values have been obtained in the chiral limit, analytically in Refs. [56] and on the lattice in Refs. [57]. However, note that lattice calculations with physical quark masses [58] have been shown to be sizably larger than the chiral limit results, suggesting that the corrections beyond the chiral limit are large [51,59].

V. ANALYTIC RESULTS

A. Sum of the 5D Witten diagrams

In this section, we show how to calculate the four-current correlators of Eqs. (67) and (68) in momentum space, i.e.

$$W_{LRLR}^{\mu\alpha\nu\beta}(p) = i^3 \lim_{l\to 0}\langle 0|T\{\tilde{L}_{\bar{s}d}^\mu(p)\tilde{R}_{\bar{d}s}^\alpha(l)\tilde{L}_{\bar{s}d}^\nu(-p)\tilde{R}_{\bar{d}s}^\beta(-l)\}|0\rangle,$$
(87)

$$W_{LLRR}^{\mu\nu\alpha\beta}(p) = i^3 \lim_{l\to 0}\langle 0|T\{\tilde{L}_{\bar{s}u}^\mu(p)\tilde{L}_{\bar{u}d}^\nu(-p)\tilde{R}_{\bar{d}u}^\alpha(l)\tilde{R}_{\bar{u}s}^\beta(-l)\}|0\rangle.$$
(88)

These expressions are in momentum space, so we use the tildes to refer to the Fourier transformed flavor currents. As we explain above, we use the vector and axial-vector field combinations, so that the vector and axial-vector currents are

$$\tilde{L}_{\bar{s}d}^\mu(p) = \tfrac{1}{\sqrt{2}}(\tilde{J}_{V,\bar{s}d}^\mu(p) + \tilde{J}_{A,\bar{s}d}^\mu(p)),$$
$$\tilde{R}_{\bar{s}d}^\mu(p) = \tfrac{1}{\sqrt{2}}(\tilde{J}_{V,\bar{s}d}^\mu(p) - \tilde{J}_{A,\bar{s}d}^\mu(p)).$$
(89)

We have the following expansion for $W_{LLRR}^{\mu\nu\alpha\beta}(p)$ in terms of the vector and axial-vector currents

$$\begin{aligned}
\frac{i^3}{4}\lim_{l\to 0}[&\tilde{J}_V^\mu(p)\tilde{J}_V^\nu(-p)\tilde{J}_V^\alpha(l)\tilde{J}_V^\beta(-l)\\
&+ \tilde{J}_V^\mu(p)\tilde{J}_V^\nu(-p)\tilde{J}_A^\alpha(l)\tilde{J}_A^\beta(-l)\\
&- \tilde{J}_A^\mu(p)\tilde{J}_V^\nu(-p)\tilde{J}_V^\alpha(l)\tilde{J}_A^\beta(-l)\\
&- \tilde{J}_A^\mu(p)\tilde{J}_V^\nu(-p)\tilde{J}_A^\alpha(l)\tilde{J}_V^\beta(-l)\\
&- \tilde{J}_V^\mu(p)\tilde{J}_A^\nu(-p)\tilde{J}_V^\alpha(l)\tilde{J}_A^\beta(-l)\\
&- \tilde{J}_V^\mu(p)\tilde{J}_A^\nu(-p)\tilde{J}_A^\alpha(l)\tilde{J}_V^\beta(-l)\\
&+ \tilde{J}_A^\mu(p)\tilde{J}_A^\nu(-p)\tilde{J}_V^\alpha(l)\tilde{J}_V^\beta(-l)\\
&+ \tilde{J}_A^\mu(p)\tilde{J}_A^\nu(-p)\tilde{J}_A^\alpha(l)\tilde{J}_A^\beta(-l)],
\end{aligned}$$
(90)

and similarly for $W_{LRLR}^{\mu\alpha\nu\beta}(p)$.

Having calculated in the previous sections the propagators for all the fields in our Lagrangian, it is a lengthy but straightforward operation to construct all of the Witten diagrams for our four-point functions. One simply uses the bulk-to-boundary propagators to connect the four boundary points together through the vertices coming from the bulk interaction Lagrangian. Connecting points inside the bulk requires a bulk-to-bulk propagator.

The inclusion of the boundary term Eq. (12) involving A_5 obviously increases the number of diagrams that contribute to any n-point function containing the axial-vector current. However, as shown in Appendix D, the Ward identities satisfied by $W_{LLRR}^{\mu\nu\alpha\beta}$ and $W_{LRLR}^{\mu\alpha\nu\beta}$ can be used to demonstrate that one gets the full result by considering purely the diagrams where only vectors and axial-vectors are connected to the boundary, and where only the transverse part of their bulk-to-boundary propagators is taken into account. This means that one need not consider the boundary term given by $A_\mu\partial_\nu A_5$ for the purpose of this paper.

For both $W_{LLRR}(Q^2)$ and $W_{LRLR}(Q^2)$, the 5D Witten diagram sum can be split into three distinct classes: diagrams where A_5 propagates in the bulk, X-diagrams involving the four-boson vertex, and Y-diagrams, which involve two three-boson vertices. Each class of diagrams contributes to the Green's functions at a different order of the momentum p: the A_5 class contributes with order p^0 and higher, the X-diagrams to order p^2 and higher, and the Y-diagrams to order p^4 and higher. We refer the reader to Appendix A for an example of each class of diagram, for the $\tilde{J}_{V,\bar{s}d}^\mu(p)\tilde{J}_{V,\bar{s}d}^\alpha(l)\tilde{J}_{A,\bar{s}d}^\nu(-p)\tilde{J}_{A,\bar{s}d}^\beta(-l)$ contribution to the W_{LRLR} correlator.[5]

Once we sum the diagrams including all the contributions, we find that the two four-point functions are proportional to each other with a factor -16. This factor comes from the $SU(3)$ group theory structure. The proportionality is strictly correct only in the $l_\alpha \to 0$ limit, which is the limit required for the computation of the g_8 and g_{27} parameters. We therefore have

$$W_{LRLR}(Q^2) = \frac{4i}{3}\frac{Q^2}{F_\pi^2}\Sigma(p=iQ),$$
(91)

$$W_{LLRR}(Q^2) = -\frac{i}{12}\frac{Q^2}{F_\pi^2}\Sigma(p=iQ),$$
(92)

where Σ denotes the sum of the diagrams and can be written as $\Sigma = \Sigma_X + \Sigma_{A_5} + \Sigma_Y$, referring to the distinct classes of diagrams. The Σ_X and Σ_{A_5} components are given by

$$\Sigma_X(p) = -i\Big(\frac{M_5 L}{2}\Big)\frac{[d-1]^3}{d}\int\frac{dz}{z}([K_0^{V^2} + K_0^{A^2}]$$
$$\times [K_p^{V^2} + K_p^{A^2}] - 4K_0^V K_0^A K_p^V K_p^A),$$
(93)

and

$$\Sigma_{A_5}(p) = -i\Big(\frac{M_5 L}{\sqrt{2}}\Big)^2\frac{[d-1]^2}{d}\int\frac{dz}{z}$$
$$\times \int\frac{dz'}{z'}G_p^5(z,z')A'(z,z'),$$
(94)

---

[5]Note that we must respect the quark-flavor contractions, which eliminates some of the Witten diagrams. We then draw all the Witten diagrams which contribute to each term in this sum, and add all the various parts. It turns out that for W_{LLRR} there are 36 distinct diagrams, which gets reduced to 24 diagrams upon enforcing the order of quark contraction. For W_{LRLR}, we find 40 such diagrams which give a nonvanishing contribution. These diagrams are the totality of *planar* diagrams when the order of quark-flavor contractions is respected.

where $d = 4$ is the dimension of spacetime and

$$A'(z, z') = 2(K_p^A \partial_z K_0^V - K_0^V \partial_z K_p^A)(K_0^A \partial_{z'} K_p^V - K_p^V \partial_{z'} K_0^A) + (K_0^A \partial_z K_p^V - K_p^V \partial_z K_0^A)(K_0^A \partial_{z'} K_p^V - K_p^V \partial_{z'} K_0^A)$$
$$+ (K_p^A \partial_z K_0^V - K_0^V \partial_z K_p^A)(K_p^A \partial_{z'} K_0^V - K_0^V \partial_{z'} K_p^A). \tag{95}$$

As for the Y-diagrams, the integrations are more involved, but the sum can be written as $\Sigma_Y(p) = Y_1 + Y_2 + Y_3 + Y_4 - 2Y_5 - 2Y_6$, where

$$Y_1 = -i\left(\frac{M_5 L}{\sqrt{2}}\right)^2 [d-1] p^2 \int \frac{dz}{z} \int \frac{dz'}{z'} K_p^V(z) G_0^V(z, z') K_p^V(z') K_0^V(z) K_0^V(z'),$$

$$Y_2 = -i\left(\frac{M_5 L}{\sqrt{2}}\right)^2 [d-1] p^2 \int \frac{dz}{z} \int \frac{dz'}{z'} K_p^V(z) G_0^A(z, z') K_p^V(z') K_0^A(z) K_0^A(z'),$$

$$Y_3 = -i\left(\frac{M_5 L}{\sqrt{2}}\right)^2 [d-1] p^2 \int \frac{dz}{z} \int \frac{dz'}{z'} K_p^A(z) G_0^A(z, z') K_p^A(z') K_0^V(z) K_0^V(z'),$$

$$Y_4 = -i\left(\frac{M_5 L}{\sqrt{2}}\right)^2 [d-1] p^2 \int \frac{dz}{z} \int \frac{dz'}{z'} K_p^A(z) G_0^V(z, z') K_p^A(z') K_0^A(z) K_0^A(z'), \tag{96}$$

$$Y_5 = -i\left(\frac{M_5 L}{\sqrt{2}}\right)^2 [d-1] p^2 \int \frac{dz}{z} \int \frac{dz'}{z'} K_p^A(z) G_0^A(z, z') K_p^V(z') K_0^V(z) K_0^A(z'),$$

$$Y_6 = -i\left(\frac{M_5 L}{\sqrt{2}}\right)^2 [d-1] p^2 \int \frac{dz}{z} \int \frac{dz'}{z'} K_p^A(z) G_0^V(z, z') K_p^V(z') K_0^A(z) K_0^V(z').$$

We perform all the integrals with the limits L_1 and L_0, and show the full results in Appendix B. The results are very complicated expressions, but one can then take the limit $L_0 \to 0$ smoothly. All the divergent contributions cancel, and we obtain the simple result

$$\Sigma(Q)_{L_0 \to 0} = 3iM_5 L\left[\frac{16}{Q^6 L_1^6} - \frac{14}{5Q^4 L_1^4} - \frac{299}{240 I_1^2}\right.$$
$$+ \frac{7}{20Q^2 L_1^2 I_1^2} + \frac{299}{240 I_0^2} - \frac{2}{15Q^2 L_1^2 I_0^2}$$
$$+ \frac{7}{5Q^4 L_1^4 I_0^2} + \frac{16}{Q^6 L_1^6 I_0^2} - \frac{32}{Q^6 L_1^6 I_0}$$
$$\left. + \frac{13}{12 Q L_1 I_0 I_1}\right], \tag{97}$$

where $I_{0,1} = I_{0,1}(QL_1)$ are the modified Bessel functions of zeroth and first order, respectively, and Q is the
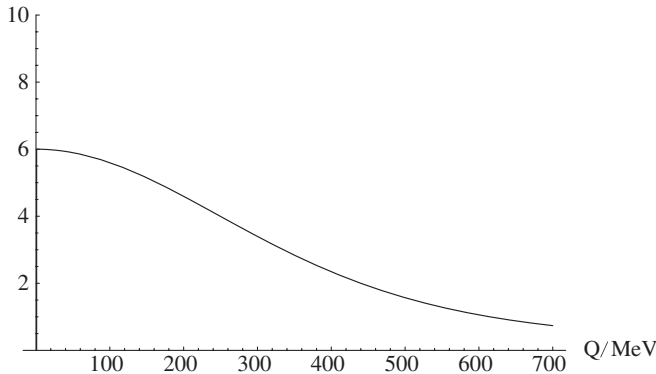

FIG. 1. A plot of W_{LRLR} against Q, in the limit $L_0 \to 0$. The correlator W_{LLRR} is -16 times smaller.

Euclidean momentum. This simplified form is more appropriate for the analysis of the high and low Q behavior of the correlators. See Fig. 1 for a plot of W_{LRLR} against momentum, with $1/L_1 = 280$ MeV. Note that W_{LRLR} is found to be positive definite, while W_{LLRR} is negative definite because of the proportionality. Both correlators also approach zero as $Q \to \infty$, and satisfy the "sum of poles" functional form of Eqs. (80) and (81). More precisely, the high Q behavior of the correlators is given by $1/Q^2$, which is the correct functional form predicted by perturbative QCD, Eqs. (78) and (79).

B. The limit $Q \to 0$ and connection with chiral perturbation theory

The pole structure of the propagators for low momentum constitutes a strong check on our calculation. Another check is whether our results agree with χPT which, as explained above, gives us a constraint on the behavior of the correlators as $Q \to 0$, Eqs. (76) and (77). Taking that limit in the expression of $\Sigma(Q)$, we obtain

$$\lim_{Q^2 \to 0} \Sigma(Q) = 3iM_5 L\left(\frac{-3}{Q^2 L_1^2} + \frac{105}{64} - \frac{1521}{2560} Q^2 L_1^2\right.$$
$$\left. + \mathcal{O}(Q^4)\right). \tag{98}$$

This is indeed the functional form required by χPT, the Q^2 pole being due to the massless pions. Our correlators therefore have the low Q behavior given by

$$\lim_{Q^2 \to 0} W_{LRLR}(Q^2) = 6 - \frac{105 M_5 L}{16} \frac{Q^2}{F_\pi^2} + \mathcal{O}(Q^4), \tag{99}$$

$$\lim_{Q^2 \to 0} W_{LLRR}(Q^2) = -\frac{3}{8} + \frac{105 M_5 L}{256} \frac{Q^2}{F_\pi^2} + \mathcal{O}(Q^4). \quad (100)$$

This is to be compared with the expressions obtained via χPT in the chiral limit, Eqs. (76) and (77). A plot of our results versus those of χPT makes things clearer, for a value of $1/L_1 = 280$ MeV (Fig. 2). The matching obtained for W_{LRLR} is very good for the range of validity of χPT, while W_{LLRR} does not exhibit as good a matching (see below). Note also that the χPT results shown in the plots do not contain any $O(p^6)$ contribution, while our 5D result is to full order in p.

In Ref. [31], the coefficients of the $\mathcal{O}(p^4)$ chiral Lagrangian were calculated in an AdS setting with identical field content to the one used in this work. This allows us to compare our predictions in the low-momentum limit to those of χPT with the AdS l_i coefficients calculated in Ref. [31]. Using those results, and the relations found between the l_i coefficients, i.e. $l_2 = 2l_1$ and $l_3 = -6l_1$, Eqs. (99) and (100) can be rewritten as

$$\lim_{Q^2 \to 0} W_{LRLR}(Q^2) = 6 - 24(2l_1 + 5l_2 + l_3 + l_9)\frac{Q^2}{F_\pi^2} + \dots \quad (101)$$

and

$$\lim_{Q^2 \to 0} W_{LLRR}(Q^2) = -\frac{3}{8} + \frac{3}{2}(l_9 - l_3)\frac{Q^2}{F_\pi^2} + \dots \quad (102)$$

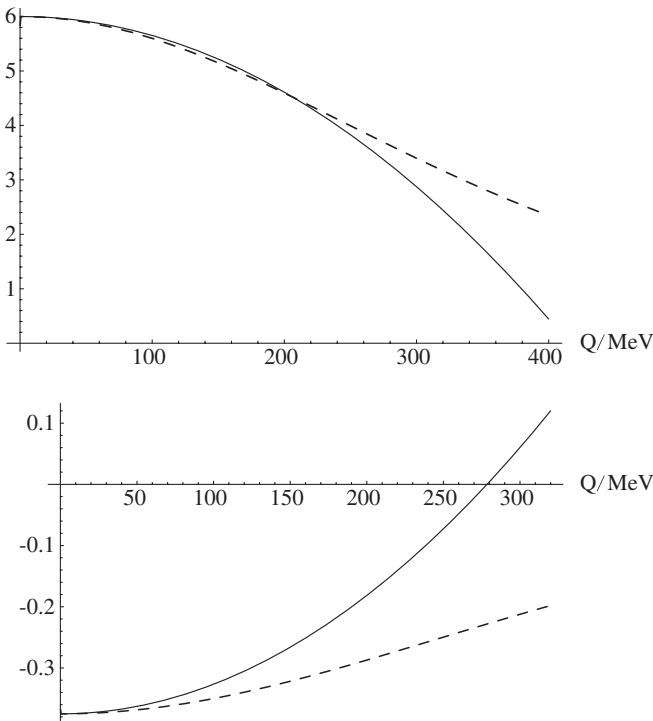Notice that the first expression coincides exactly with the

FIG. 2. The low Q behavior of W_{LRLR} (top) and W_{LLRR} (bottom) in the $L_0 \to 0$ limit: the dashed line is the AdS prediction, the solid line is χPT.

pure χPT calculation, Eq. (76). Similarly, for W_{LLRR}, the $O(p^2)$ coefficient $-3/8$ and the $O(p^4)$ l_9 coefficient $+3/2$ coincide with the corresponding coefficients of Eq. (77). However, the holographic calculation does not reproduce the $O(p^4)$ l_3 coefficient of Eq. (77), yielding a factor $-3/2$ in place of $-15/2$, so that the total Q^2 coefficient in W_{LLRR} differs by a factor two approximately from the χPT result. We do not understand this discrepancy. We have performed a variety of consistency checks on the 5D calculation, and we do not see any possibility of deviations which would alter the proportionality between W_{LLRR} and W_{LRLR}. This makes us confident that our results are correct. It seems possible to us that the problem might lie with the sole and rather subtle χPT calculation of the l_3 dependence of W_{LLRR}. Note also that this difference in the l_3 coefficient for W_{LLRR} is not significant enough to alter the fact that we find a large enhancement for g_8 below.

VI. NUMERICAL RESULTS AND DISCUSSION

In this section we present our numerical results for the $\Delta I = 1/2$ rule and the B_K mixing parameter. To obtain the values of the parameters g_8 and g_{27}, we must integrate the two four-current correlators over the Euclidean momentum as explained in Eqs. (69)–(71). This integral should ideally be regularized in the same scheme as the Wilson coefficients of the four-quark operators responsible for the kaon decay. These are z_1 and z_2, and they are usually renormalized using dimensional regularization in three distinct schemes: leading order (LO), t'Hooft-Veltman (HV), and naive dimensional regularisation (NDR). On the other hand, the sharp UV boundary at $z = L_0$ in the 5D calculation implies that a hard cutoff at scale $1/L_0$ should be employed in the momentum integral, and that one should use the appropriate values of the Wilson coefficients z_1 and z_2 at this energy scale. We therefore focus upon the Wilson coefficients calculated in the LO renormalization scheme as this provides a closer, though admittedly not exact, match to the holographic part of the calculation. One may justify this choice as follows: our results for the correlators have the functional form expected from QCD calculations in Eqs. (78) and (79). The integrals carried out in the computation of g_8 and g_{27} will therefore have a logarithmic divergence with respect to the cutoff, rendering the integration stable under changes of the high-momentum scale.

We employ two choices of the high-momentum cutoff: 1300 MeV, which is approximately the mass of the charm quark, and 1500 MeV.[6] Below, we also demonstrate that

---

[6]In taking the cutoff to be 1500 MeV, which is above the charm threshold, we should also consider the contribution of four-quark operators involving the charm quark (see. e.g. [60]). However, for a scale not larger than 1500 MeV, which is well below the mass of the charmed resonances, their contribution is expected to be quite small, and in the following we neglect them.

the results of our calculation are stable against changes in this cutoff. The values of the Wilson coefficients z_1 and z_2 that we use, as calculated in the work of [60] for the LO scheme, are $z_1 = -0.625$, $z_2 = 1.345$, at 1300 MeV and $z_1 = -0.5699$, $z_2 = 1.307$, at 1500 MeV. For $C_{\Delta S=2}$ we use the values 1.17 and 1.21, respectively.

Below, we employ a self-consistent prescription to carry out two distinct fits. In the first, we fit to the following observables: the mass of the rho meson m_ρ, the mass of the a_1 axial-vector meson m_{a_1}, F_π, g_8, and g_{27}. The values of F_π, $m_\rho^{\rm exp}$, and $m_{a_1}^{\rm exp}$ that we fit to are 87 MeV, 776 MeV, and 1230 MeV, respectively. For g_8 and g_{27}, as explained in Sec. IV, the values we fit to are $g_8 = 3.3$ and $g_{27} = 0.23$, equivalent to $g_8^{\rm TOT} = g_8 + g_8^{\rm HO} = 5.1$, and $g_{27}^{\rm TOT} = g_{27} + g_{27}^{\rm HO} = 0.29$, Eqs. (65) and (66). In the second type of fit, we fit to ω and B_K instead of g_8 and g_{27}, taking the values $\omega = 1/22.2$ and $\hat{B}_K = 0.36$, see Sec. IV. The only free parameters in both fits are $M_5 L$ and L_1. Inside the integral, we use our full result for finite L_0, the Minkowski version of which is shown in Appendix B. The predictions of the model for F_π, m_ρ, and m_{a_1}, entering in the fits, are [29–31,37]

$$F_\pi^{\rm th} = \sqrt{\frac{2M_5 L}{L_1^2 - L_0^2}}, \qquad (103)$$

and, to a good approximation in the range of interest,

$$m_\rho^{\rm th} \approx \frac{2.12}{L_1} \frac{(L_1 - 0.282 L_0)}{(L_1 - L_0)}, \qquad (104)$$

$$m_{a_1}^{\rm th} \approx \frac{3.38}{L_1} \frac{(L_1 - 0.085 L_0)}{(L_1 - L_0)}. \qquad (105)$$

The results for both fits are given in Table I and are quite similar. Taking into account the relative crudeness of our model, and the use of the large-N_c expansion of QCD, we find these results quite good. The discrepancy with experi-

TABLE I.　Columns *A*, *B* show a fitting to m_ρ, m_{a_1}, F_π, g_8, and g_{27}. Columns C, D show a fitting to m_ρ, m_{a_1}, F_π, $1/\omega$, and $\hat{B}_K$. Note that, as explained in Sec. IV, $g_8^{\rm TOT} = g_8 + 1.8$, $g_{27}^{\rm TOT} = g_{27} + 0.06$, where g_8 and g_{27} are the quantities we calculated from the AdS model. We use the values $F_\pi = 87$ MeV, $m_\rho^{\rm exp} = 776$ MeV, $m_{a_1}^{\rm exp} = 1230$ MeV, $g_8^{\rm exp} = 5.1$, and $g_{27}^{\rm exp} = 0.29$.

Observable	A	B	C	D
L_0^{-1}	1300 MeV	1500 MeV	1300 MeV	1500 MeV
L_1^{-1}	274 MeV	275 MeV	277 MeV	280 MeV
$m_\rho^{\rm th}/m_\rho^{\rm exp}$	0.91	0.90	0.93	0.92
$m_{a_1}^{\rm th}/m_{a_1}^{\rm exp}$	0.95	0.93	0.97	0.95
$F_\pi^{\rm th}/F_\pi$	1.15	1.17	1.12	1.14
$g_8^{\rm TOT}/g_8^{\rm exp}$	0.74	0.72	0.75	0.74
$g_{27}^{\rm TOT}/g_{27}^{\rm exp}$	0.85	0.85	0.79	0.78
$1/\omega$	19.5	19.2	21.4	21.3
$\hat{B}_K^{\rm th}$	0.38	0.38	0.34	0.34

ment never exceeds $\sim 25\%$, and for some observables is much smaller. It must be emphasized again that, having picked the values for the upper cutoff to be 1300 MeV and 1500 MeV and thereby fixed L_0, the only remaining free parameters are L_1 and $M_5 L$. Therefore, we fit five independent observables with only two free parameters.

To understand the structure of the g_8 and g_{27} results in Table I, it is useful to decompose the numerical results into three components: the leading N_c factorized part of Eqs. (69)–(71) given explicitly in Eqs. (74) and (75), the $1/N_c$ nonfactorizable contribution of Eqs. (69)–(71) (encoded in the W_{LRLR} and W_{LLRR} Green's functions we calculated), and the contribution from the higher-order corrections, $g_8^{\rm HO}$ and $g_{27}^{\rm HO}$, which as said above we take from Ref. [41]. For example, for the results of column A this decomposition goes as follows: $g_8^{\rm TOT} = 1.06 + 0.92 + 1.8 = 3.78$ and $g_{27}^{\rm TOT} = 0.43 - 0.24 + 0.06 = 0.25$, whereas the experimental values to compare with are $g_8^{\rm exp} = 5.1$ and $g_{27}^{\rm exp} = 0.29$, respectively. We see that, for g_8, the nonfactorizable chiral limit contribution of 0.92 is of the same order as the factorized contribution of 1.06, and effectively doubles it. For g_{27}, the nonfactorizable contribution of -0.24 effectively divides the factorized result of 0.43 by more than two. As already mentioned above, the fact that the $1/N_c$ contribution can be as large as the factorized part, even though the $1/N_c$ series is still expected to converge, can be naturally explained by the interplay of the various hadronic scales involved in g_8 and g_{27} [36].

For a rather conservative estimate of the error[7] involved in our calculation, it is interesting to compare the results of Table I with the values we obtain by fitting only F_π, m_ρ, and m_{a_1}. In this case, for example, with $L_0^{-1} = 1300$ MeV, we get $F_\pi^{\rm th}/F_\pi^{\rm exp} = 1.00$, $m_\rho^{\rm th}/m_\rho^{\rm exp} = 0.98$, $m_{a_1}^{\rm th}/m_{a_1}^{\rm exp} = 1.02$, and $g_8^{\rm TOT} = 1.06 + 1.32 + 1.8 = 4.18$, which gives $g_8^{\rm TOT}/g_8^{\rm exp} = 0.82$. In this case, the nonfactorizable chiral limit contribution of 1.32, is $\sim 40\%$ larger than the value 0.92 above. For g_{27} we get a smaller result: $g_{27}^{\rm TOT} = 0.43 - 0.35 + 0.06 = 0.14$, so that the nonfactorizable chiral limit contribution of -0.35, is also $\sim 40\%$ larger than the value -0.24 above. The small total result it gives is not surprising, as g_{27} involves the difference of two large positive contributions, i.e. a $1/N_c^2$ correction of order $\sim 30\%$ of our $1/N_c$ contribution would bring g_{27} close to the experimental value.

Note that our results are similar to what has been obtained in other analytical calculations utilizing the $1/N_c$ expansion [36,48,49]. In particular, in Ref. [36] the values $g_8^{\rm TOT}/g_8^{\rm exp} = 0.76$ and $g_{27}^{\rm TOT}/g_{27}^{\rm exp} = 0.79$ have been obtained. The two methods are, however, quite different, as explained in Sec. IV. The main advantage of our model is that it allows the calculation of the four-point functions in

---

[7]This is also useful as an estimate of higher-order $1/N_c$ correction effects.

the entire relevant momentum region within one consistent setting, thereby removing the need for interpolation in any specific momentum range.

One could ask why we took the parameter M_5L as a free parameter in the fits. In Refs. [29–33,37,61], it has been shown that this parameter determines the high Q^2 logarithm of the vector-current two-point correlator, so that it can be fixed from a matching with the corresponding QCD coefficient [62], yielding

$$M_5L = \frac{N_c}{12\pi^2}. \qquad (106)$$

The point is that, for two-point functions only, there is enough parameter freedom to match the QCD logarithm (see in particular [29–31]), unlike the more complicated case presented here. Clearly, it is not expected that the model we consider, based on a simple slice of AdS with a hard cutoff in the UV at the scale L_0^{-1}, would lead to the exactly correct QCD behavior. However, comparing our results with those of QCD in Eqs. (78) and (79), we observe that for both W_{LRLR} and W_{LLRR} we reproduce the good functional behavior (i.e. the $1/Q^2$ dependence). We also observe that we get the correct sign for the coefficients of $1/Q^2$ and, amazingly, we even get values for these coefficients which are within a factor 2–3 of the perturbative QCD result, for $Q^2 \sim 2$–5 GeV^2. Note that this is a very surprising outcome, especially for W_{LLRR}, because the high-momentum dependence of the latter involves the quark condensate contribution, as seen in Eq. (79). In fact, the dominance of the quark condensate term in Eq. (79) guarantees that W_{LLRR} is negative in the far UV, and so we predict its sign correctly, although our model has no equivalent of the quark condensate (or of α_s for that matter). As mentioned above, one way of introducing a tunable condensate is by adding a scalar field in the bulk. It would be interesting to see whether the calculation of W_{LLRR} in that case gives a more accurate description of the high-momentum behavior.

We showed in Sec. III A that the 5D bulk Lagrangian we employ is the leading order Lagrangian in the large-N_c expansion, and that operators of higher mass dimension are subleading in N_c. In principle, these operators may contribute to the four-point functions calculated here. In this section, we have presented the results of a fit of five observables using only two independent parameters, which are the IR brane position L_1 and the dimensionless combination M_5L. Thus, the fact that a fit using only the leading operator of Eq. (2) gives good agreement to the data is nontrivial. If we were to introduce the full set of subleading operators that contribute, then we increase the number of free parameters of the model (because the coefficients of the new operators are unconstrained by bulk gauge invariance or other symmetries) and the fit loses predictivity. Therefore, the success of the restricted fit performed here shows that the coefficients of the subleading operators are not anomalously large.

A technical, but important, issue to mention concerns the gauge symmetry of the 5D theory. To carry out the 5D calculations, we had to choose a specific gauge to work in, and we picked the convenient R_ξ gauge taken in the limit $\xi \to \infty$. Now, it is clear that the results of the holographic calculation must be independent of the gauge parameter ξ, and of any choice of gauge fixing. This must, in fact, be a feature of any holographic calculation involving gauge freedom in the AdS theory. In previous AdS/QCD computations there had been no need for concern, since these calculations only involved two-point functions and all the propagators in the 5D theory were boundary-to-boundary ones. Boundary-theory current conservation then automatically projects out the longitudinal gauge-dependent component of the 5D propagators, rendering the results gauge independent. Unfortunately, the situation is less clear in the case of four-current correlators, because the latter involve Witten diagrams with explicitly gauge-dependent propagators (exchange diagrams [38]). In the above, we trust that the power of AdS/CFT guarantees that any such holographic calculation will yield results that are independent of the 5D gauge fixing.

The model has many shortcomings, due to its crude nature. For example, a concern for this class of models is the behavior of the masses of the resonances M_{V_n} and M_{A_n} as n approaches infinity. One finds that the simple treatment presented here shows that the masses of the Kaluza-Klein modes go like n for large n, in sharp contrast to the predictions of large-N_c theories, in which the masses of the resonances go like $\sqrt{n}$. A recent paper [63] has shown, however, that with a more sophisticated handling of the IR truncation of the AdS space, one can indeed recover the large-N_c Regge behavior. Whether this will improve the results obtained here remains to be seen. Finally, one must keep in mind that the calculations done here were all in the chiral limit. In order to account for massive quarks, one would have to introduce the bi-fundamental scalar of Refs. [29,30]. In particular, this would allow the inclusion of the mass of the strange quark, whose effect could easily be as large as 20%–25% for g_8, or even more for g_{27}, due to the cancellation of factorizable and nonfactorizable contributions in the latter.

VII. CONCLUSIONS

In this paper we have calculated, within the simplest possible version of holographic QCD, the four-point flavor current correlators crucial to the resolution of the $\Delta I = 1/2$ puzzle of QCD. We believe that our results are quite encouraging for the AdS/QCD approach. The holographic theory automatically and consistently includes the contributions of the infinite tower of meson resonances to the four-point correlators. We also reproduce, to a good level of accuracy, the low-momentum and high-momentum behavior of these correlators, as deduced from chiral perturbation theory and perturbative QCD, respectively. This

agreement is particularly impressive for the correlator W_{LRLR}. Moreover, the results of a fit of the holographic predictions to the experimental data agree well, with 25% accuracy or better, showing that the dynamics of the $\Delta = 1/2$ rule is operative in AdS/QCD. For quantities as difficult to calculate as the isospin amplitudes of kaon decay $\mathrm{Re}A_0$ and $\mathrm{Re}A_2$, this is remarkable.

A rather obvious limitation of the model concerns the description of χSB. As explained above, although the imposition of IR boundary conditions on the bulk $SU(3)_L \times SU(3)_R$ gauge fields correctly incorporates the leading χSB behavior, a bi-fundamental bulk scalar is needed to fully account for the physics of χSB. The inclusion of this field will directly introduce pseudoscalar resonances into the 4D field content, and these will indeed have relevant contributions to the four-current correlators calculated here. We will also have an extra parameter that can be tuned [29,30], corresponding to the quark condensate. We have also not included the effects of the anomalous $U(1)_A$ symmetry of QCD, nor the explicit breaking of chiral symmetry due to bare quark masses. One envisions these improvements having a complicated yet positive effect on the calculation of four-point current correlators presented in this paper.

We believe that the results of this paper for four-point functions show that it is worth investigating further the predictions of AdS/QCD.

## APPENDIX A: THE DIFFERENT CLASSES OF 5D WITTEN DIAGRAMS

We adopt the following conventions in labeling the vector, axial-vector, and pseudoscalar propagators:

Using the vertices calculated from the full Lagrangian, we can then draw all the Feynman diagrams that contribute to a specific four-point function in momentum space. To illustrate this, we consider here the $\langle J_V J_V J_A J_A \rangle$ piece contributing to W_{LRLR}. This is given by the following sum of diagrams:
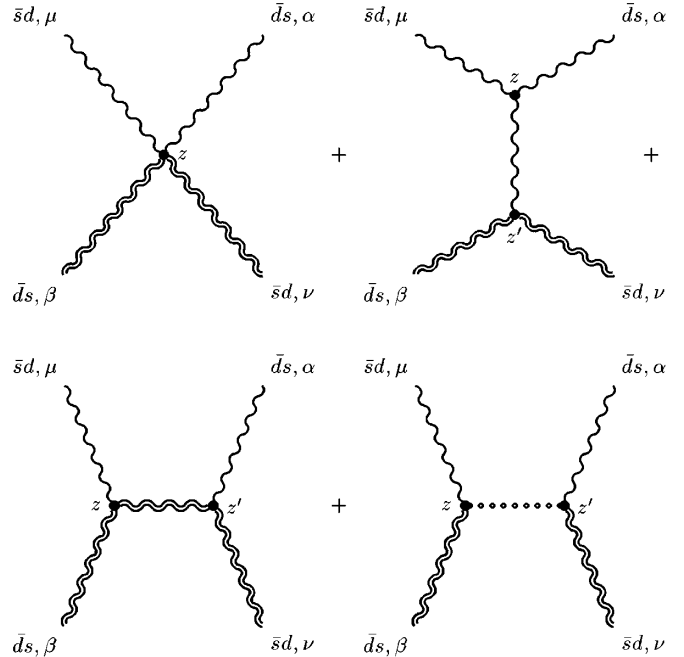
In principle, one could have two more "cross diagrams," but they are eliminated by the large-N_c condition that diagrams must be planar.

APPENDIX B: THE SUM OF WITTEN DIAGRAMS FOR FINITE L_0

Here we present the results of the Witten diagram summation for finite L_0 in Minkowski space. As in Sec. V, we write $\Sigma = \Sigma_X + \Sigma_{A_5} + \Sigma_Y$. Defining

$$C_n(z) = C\mathcal{J}_n(pz) + D\mathcal{Y}_n(pz),$$
$$\bar{C}_n(z) = \bar{C}\mathcal{J}_n(pz) + \bar{D}\mathcal{Y}_n(pz),$$
$$F(z) = p^2[z^2 C_2(z) + L_1^2 C_0(z)],$$
$$G(z) = p^4 z^4 C_2(z) - 2p^3 z^3 C_3(z) - p^4 L_1^2 z^2 C_2(z)$$

we obtain

$$\Sigma_{A_5} = \frac{36iM_5 L}{L_0^2(L_1^2 - L_0^2)^3(AD - BC)^2 p^4}([z^2 C_2(z)]|_{L_0}^{L_1})^2,$$

and

$$\Sigma_X = 3iM_5\left(\frac{9}{8}\right)\left[\frac{1}{L_0^2(AD-BC)^2}\left(\frac{z^2}{2}(C_1(z)^2 - C_0(z)C_2(z))\right) + \frac{1}{L_0^2(A\bar{D}-B\bar{C})^2}\left(\frac{z^2}{2}(\bar{C}_1(z)^2 - \bar{C}_0(z)\bar{C}_2(z))\right)\right.$$

$$+ \frac{1}{L_0^2(L_1^2 - L_0^2)^2(AD-BC)^2}\left(\frac{-z^4(\frac{6}{5p^2}+L_1^2)}{3}(C_1(z)^2 + C_2(z)^2) + \frac{L_1^4 z^2}{2}(C_1(z)^2 - C_0(z)C_2(z))\right.$$

$$+ \frac{z^4}{10p^2}\left((p^2z^2+3)C_1(z)^2 + \frac{p^2z^2}{4}(C_0(z)+3C_2(z))^2\right)\bigg) + \frac{1}{L_0^2(L_1^2-L_0^2)^2(A\bar{D}-B\bar{C})^2}\left(\frac{-z^4(\frac{6}{5p^2}+L_1^2)}{3}(\bar{C}_1(z)^2\right.$$

$$+ \bar{C}_2(z)^2) + \frac{L_1^4 z^2}{2}(\bar{C}_1(z)^2 - \bar{C}_0(z)\bar{C}_2(z)) + \frac{z^4}{10p^2}\left((p^2z^2+3)\bar{C}_1(z)^2 + \frac{p^2z^2}{4}(\bar{C}_0(z)+3\bar{C}_2(z))^2\right)\bigg)$$

$$+ \frac{4}{L_0^2(L_1^2-L_0^2)(AD-BC)(A\bar{D}-B\bar{C})}\left(\frac{z^4}{6}C_2(z)\bar{C}_2(z) + \left(\frac{z^4}{6}-\frac{L_1^2 z^2}{2}\right)C_1(z)\bar{C}_1(z) + \frac{L_1^2 z^2}{4}(C_0(z)\bar{C}_2(z)\right.$$

$$\left.\left.+ C_2(z)\bar{C}_0(z))\right)\right]_{L_0}^{L_1}.$$

Writing $\Sigma_Y(p) = Y_1 + Y_2 + Y_3 + Y_4 - 2Y_5 - 2Y_6$, we obtain

$$Y_1 = \frac{3iM_5 L}{4L_0^2(AD-BC)^2}([z^2 C_1(z)^2]_{L_0}^{L_1} - L_0^2 C_0(L_0)^2),$$

$$Y_2 = \frac{3iM_5 L p^2}{4L_0^2(L_0^2-L_1^2)^3(AD-BC)^2}\left(\frac{L_1^2-L_0^2}{p^8}\left[\frac{p^6 z^6}{5}[C_1(z)C_3(z)+C_2(z)C_4(z)] + \frac{p^6 z^4 L_1^2}{3}[C_1(z)^2 + C_2(z)^2]\right.\right.$$

$$-L_1^4 p^6 z^2[C_1(z)^2 - C_0(z)C_2(z)] - 2p^2 L_1^2\left(C_0(z)[p^3 z^3 C_1(z) - 4p^2 z^2 C_2(z)] + \frac{p^4 z^4}{6}[C_0(z)C_2(z)+C_1(z)C_3(z)]\right)\bigg]_{L_0}^{L_1}$$

$$+ \frac{1}{p^8}[(L_0^2 F(L_0) - L_1^2 F(L_1))(G(L_1)-G(L_0)) - (L_0^2 G(L_1) - L_1^2 G(L_0))(F(L_1)-F(L_0))]$$

$$+ \frac{1}{p^{10}}(G(L_1)-G(L_0))^2 + \frac{L_0^2 L_1^2}{p^6}(F(L_1)-F(L_0))^2\bigg),$$

$$Y_3 = \frac{3iM_5 L}{4L_0^2(L_0^2-L_1^2)(A\bar{D}-B\bar{C})^2 p^4}[p^4 L_1^2(L_1^2-L_0^2)\bar{C}_0(L_1)\bar{C}_2(L_1) + p^4 L_0^2(L_1^2-L_0^2)[\bar{C}_0(L_0)^2 + \bar{C}_1(L_0)^2] + 4p^2 L_0^2\bar{C}_1(L_0)^2],$$

$$Y_4 = \frac{3iM_5 L p^2}{4L_0^2(L_1^2-L_0^2)^2(A\bar{D}-B\bar{C})^2}\left(\left[-\frac{z^6}{5p^2}[\bar{C}_1(z)\bar{C}_3(z)+\bar{C}_2(z)\bar{C}_4(z)] + \frac{L_1^2 z^4}{3p^2}[\bar{C}_1(z)(\bar{C}_3(z)-\bar{C}_1(z)) + \bar{C}_2(z)(\bar{C}_0(z)-\bar{C}_2(z))]\right]_{L_0}^{L_1}\right.$$

$$-\frac{L_1^6}{p^2}\bar{C}_0(L_1)\bar{C}_2(L_1) - 2\frac{L_1^5}{p^3}\bar{C}_0(L_1)\bar{C}_3(L_1) - \frac{L_1^4 L_0^2}{p^2}[\bar{C}_1(L_0)^2 + \bar{C}_0(L_0)^2] - 2\frac{L_0^3}{p^3}\bar{C}_2(L_0)[L_0^2\bar{C}_3(L_0)+L_1^2\bar{C}_1(L_0)]\bigg),$$

$$Y_5 = \frac{3iM_5 L p^2}{4L_0^2(L_1^2-L_0^2)^2(A\bar{D}-B\bar{C})(AD-BC)}\left[2\frac{(L_0^2-L_1^2)}{p^2}\left(\frac{z^4}{6}[\bar{C}_1(z)C_1(z)+\bar{C}_2(z)C_2(z)]\right.\right.$$

$$\left.-\frac{z^2 L_1^2}{4}[2\bar{C}_1(z)C_1(z) - \bar{C}_2(z)C_0(z) - \bar{C}_0(z)C_2(z)]\right) - 2\frac{L_0\bar{C}_1(L_0)}{p^7}[G(z)-p^2 L_1^2 F(z)]\bigg]_{L_0}^{L_1},$$

$$Y_6 = \frac{3iM_5 L p^2}{4L_0^2(L_0^2-L_1^2)(A\bar{D}-B\bar{C})(AD-BC)}\left(\frac{2L_0 C_0(L_0)}{p^3}[L_0^2\bar{C}_3(L_0) + L_1^2\bar{C}_1(L_0)]\right.$$

$$+ \frac{1}{p^6}\left[\frac{p^4 L_1^4}{3}C_2(L_1)\bar{C}_2(L_1) + 2p^3 L_1^3 C_1(L_1)\bar{C}_0(L_1) + \frac{1}{2}(8+p^2 L_1^2)p^2 L_1^2 C_2(L_1)\bar{C}_0(L_1)\right.$$

$$+ \frac{1}{2}(8+p^2 L_1^2)p^2 L_0^2[2C_1(L_0)\bar{C}_1(L_0) - C_0(L_0)\bar{C}_2(L_0) - C_2(L_0)\bar{C}_0(L_0)]$$

$$\left.\left.-\frac{p^4 L_0^4}{3}[C_1(L_0)\bar{C}_1(L_0)+C_2(L_0)\bar{C}_2(L_0)] - 2p^3 L_0^3[C_1(L_0)\bar{C}_0(L_0)+C_2(L_0)\bar{C}_1(L_0)]\right]\right).$$

APPENDIX C: THE AXIAL TWO-POINT FUNCTION

The axial two-point function is defined by

$$\langle J_A^\mu(x) J_A^\nu(x') \rangle = -i \int d^4 p \, e^{-ip(x-x')} \Pi_A^{\mu\nu}(p).$$

The Ward identities require a transversal $\Pi_A^{\mu\nu}(p)$, so that we may write $\Pi_A^{\mu\nu}(p) = \Pi_A(p^2) T^{\mu\nu}$, where $T^{\mu\nu}$ is the transversal projector in p. To calculate this two-point function in our AdS/QCD setup, we have to use the boundary Lagrangian as shown in Eq. (12). This allows us to write an expression for the axial current by differentiating the full Lagrangian with respect to the boundary source a_μ. Schematically, we obtain the following expression

$$J_A^\mu(x) = \frac{M_5 L}{z} \left[-\partial_z A_\mu(x, z) + \partial_\mu A_5(x, z) \right]_{L_0}.$$

Plugging this expression into the equation for the axial two-point function, we find that we can write the result as the sum of the propagators of the A_μ and A_5 fields, giving

$$\langle J_A^\mu(x) J_A^\nu(x') \rangle = \frac{M_5 L}{z'} \partial_{z'} \left(\frac{M_5 L}{z} \partial_z \langle A_\mu(x, z) A_\nu(x' z') \rangle \right) \Big|_{z, z' = L_0}$$
$$+ \left(\frac{M_5 L}{L_0} \right)^2 \partial'_\mu \partial_\nu \langle A_5(x, L_0) A_5(x', L_0) \rangle.$$

Now, making use of the definitions of the axial propagators found in Sec. V above, it is easy to see that the A_5 propagator cancels the longitudinal part of the A_μ bulk-to-boundary propagator. Thus, the boundary term containing A_5 is essential for the satisfaction of the transversality condition.

APPENDIX D: SIMPLIFICATION TO TRANSVERSE BOUNDARY PROPAGATORS

The proof that only the transverse part of the boundary propagators is necessary for the calculation of $W_{LLRR}(Q^2)$ and $W_{LRLR}(Q^2)$ is as follows: Consider a general four-point function with external momenta p_μ, p_ν, l_α, and l_β. We assume the most general boundary propagators, i.e. with transverse and longitudinal parts. We can write this general four-point function as

$$W_4^{\mu\nu\alpha\beta} = c_1 T^\alpha T^\beta T^\mu T^\nu + d_1 T^\alpha T^\beta T^\mu p^\nu + d_2 T^\alpha T^\beta p^\mu T^\nu + d_3 T^\alpha l^\beta T^\mu T^\nu + d_4 l^\alpha T^\beta T^\mu T^\nu + e_1 T^\alpha T^\beta p^\mu p^\nu$$
$$+ e_2 l^\alpha l^\beta T^\mu T^\nu + e_3 T^\alpha l^\beta T^\mu p^\nu + e_4 T^\alpha l^\beta p^\mu T^\nu + e_5 l^\alpha T^\beta p^\mu T^\nu + e_6 l^\alpha T^\beta T^\mu p^\nu + f_1 T^\alpha l^\beta p^\mu p^\nu$$
$$+ f_2 l^\alpha T^\beta p^\mu p^\nu + f_3 l^\alpha l^\beta T^\mu p^\nu + f_4 l^\alpha l^\beta p^\mu T^\nu + g_1 l^\alpha l^\beta p^\mu p^\nu.$$

In this expression, T^μ and T^ν are transverse projectors in p^μ and p^ν, respectively, whereas T^α and T^β are transverse projectors in l^α and l^β. We omit the second index of every transverse projector, since it is contracted inside the coefficient functions $c_i \rightarrow g_i$, where all the vertex and gauge structure resides. For instance, $d_1 T^\alpha T^\beta T^\mu p^\nu$ is really $d_{1, \alpha'\beta'\mu'\nu'} T^{\alpha\alpha'} T^{\beta\beta'} T^{\mu\mu'} p^\nu p^{\nu'}$, where this term can originate from the longitudinal part of a bulk-to-boundary vector or axial-vector propagator, or from an A_5 particle emitted from an axial-vector current at the boundary. Now, the Ward identities obeyed by the four-point functions calculated above are

$$l_\alpha l_\beta W_4^{\mu\nu\alpha\beta} = 0 \quad \text{and} \quad p_\mu p_\nu W_4^{\mu\nu\alpha\beta} = 0.$$

Applying the first Ward identity to the general form for the correlator, we obtain that

$$e_2 T^\mu T^\nu + g_1 p^\mu p^\nu + f_4 p^\mu T^\nu + f_3 T^\mu p^\nu = 0.$$

But this can only mean that each term in this equation separately vanishes, because these terms are linearly independent. Arguing similarly, one can apply the second Ward identity to find that the coefficients which must be zero are $e_1, e_2, f_1, f_2, f_3, f_4$, and g_1. Now, what we are really after is the Lorentz singlet quantity given by the contraction of $W_4^{\mu\nu\alpha\beta}$ with $\eta_{\mu\nu} \eta_{\alpha\beta}$ (the equivalent of $W_{LLRR}(Q^2)$ and $W_{LRLR}(Q^2)$). This contraction trivially removes all the remaining nonzero terms, apart from the c_1 term, which is precisely the one composed entirely of transverse external propagators. Thus, we have shown that the only term that contributes to the scalar functions $W_{LLRR}(Q^2)$ and $W_{LRLR}(Q^2)$ is the one obtained by using the transverse propagators only on the external lines of the Witten diagrams.

[1] J. M. Maldacena, Adv. Theor. Math. Phys. **2**, 231 (1998).

[2] S. S. Gubser, I. R. Klebanov, and A. M. Polyakov, Phys. Lett. B **428**, 105 (1998).

[3] E. Witten, Adv. Theor. Math. Phys. **2**, 253 (1998).

[4] For a review, see e.g. O. Aharony, S. S. Gubser, J. M. Maldacena, H. Ooguri, and Y. Oz, Phys. Rep. **323**, 183 (2000).

[5] M. Kruczenski, D. Mateos, R. C. Myers, and D. J. Winters, J. High Energy Phys. 07 (2003) 049.

[6] J. Babington, J. Erdmenger, N. J. Evans, Z. Guralnik, and I. Kirsch, Phys. Rev. D **69**, 066007 (2004).

[7] M. Kruczenski, D. Mateos, R. C. Myers, and D. J. Winters, J. High Energy Phys. 05 (2004) 041.

[8] J. Babington, J. Erdmenger, N. J. Evans, Z. Guralnik, and I. Kirsch, Fortschr. Phys. **52**, 578 (2004).

[9] T. Sakai and S. Sugimoto, Prog. Theor. Phys. **113**, 843 (2005).

[10] G. F. de Teramond and S. J. Brodsky, Phys. Rev. Lett. **94**, 201601 (2005).

[11] S. Hong, S. Yoon, and M. J. Strassler, arXiv:hep-ph/0501197.

[12] T. Sakai and S. Sugimoto, Prog. Theor. Phys. **114**, 1083 (2005).

[13] G. F. de Teramond and S. J. Brodsky, arXiv:hep-ph/0507273.

[14] I. R. Klebanov, Int. J. Mod. Phys. A **21**, 1831 (2006).

[15] R. Apreda, J. Erdmenger, and N. Evans, J. High Energy Phys. 05 (2006) 011.

[16] S. J. Brodsky and G. F. de Teramond, AIP Conf. Proc. **814**, 108 (2006).

[17] K. Ghoroku, N. Maru, M. Tachibana, and M. Yahiro, Phys. Lett. B **633**, 602 (2006).

[18] K. Peeters, J. Sonnenschein, and M. Zamaklar, J. High Energy Phys. 02 (2006) 009.

[19] G. T. Horowitz and J. Polchinski, arXiv:gr-qc/0602037.

[20] N. Evans and T. Waterson, J. High Energy Phys. 01 (2007) 058.

[21] J. Erdmenger, N. Evans, and J. Grosse, J. High Energy Phys. 01 (2007) 098.

[22] E. Antonyan, J. A. Harvey, and D. Kutasov, Nucl. Phys. **B776**, 93 (2007).

[23] N. Evans and A. Tedder, Phys. Lett. B **642**, 546 (2006).

[24] J. Polchinski and M. J. Strassler, Phys. Rev. Lett. **88**, 031601 (2002).

[25] R. C. Brower and C. I. Tan, Nucl. Phys. **B662**, 393 (2003).

[26] J. Polchinski and M. J. Strassler, J. High Energy Phys. 05 (2003) 012.

[27] S. J. Brodsky and G. F. de Teramond, Phys. Lett. B **582**, 211 (2004).

[28] R. C. Brower, J. Polchinski, M. J. Strassler, and C. I. Tan, arXiv:hep-th/0603115.

[29] J. Erlich, E. Katz, D. T. Son, and M. A. Stephanov, Phys. Rev. Lett. **95**, 261602 (2005).

[30] L. Da Rold and A. Pomarol, Nucl. Phys. **B721**, 79 (2005).

[31] J. Hirn and V. Sanz, J. High Energy Phys. 12 (2005) 030; arXiv:hep-ph/0510023.

[32] L. Da Rold and A. Pomarol, J. High Energy Phys. 01 (2006) 157.

[33] E. Katz, A. Lewandowski, and M. D. Schwartz, Phys. Rev. D **74**, 086004 (2006).

[34] J. P. Shock and F. Wu, J. High Energy Phys. 08 (2006) 023.

[35] E. Shuryak, arXiv:hep-th/0605219.

[36] T. Hambye, S. Peris, and E. de Rafael, J. High Energy Phys. 05 (2003) 027.

[37] T. Hambye, B. Hassanain, J. March-Russell, and M.

[38] Schvellinger, Phys. Rev. D **74**, 026003 (2006).

[38] See e.g. D'Hoker, Eric Freedman, and Z. Daniel, arXiv:hep-th/0201253, and references therein.

[39] L. Randall and M. D. Schwartz, J. High Energy Phys. 11 (2001) 003.

[40] M. Abramowitz and I. A. Stegun, *Handbook of Mathematical Functions* (Dover, New York, 1972).

[41] J. Kambor, J. Missimer, and D. Wyler, Phys. Lett. B **261**, 496 (1991); J. Kambor, J. F. Donoghue, B. R. Holstein, J. Missimer, and D. Wyler, Phys. Rev. Lett. **68**, 1818 (1992); E. Pallente, A. Pich, and I. Scimemi, Nucl. Phys. **B617**, 441 (2001); J. Bijnens, P. Dhonte, and F. Persson, Nucl. Phys. **B648**, 317 (2003).

[42] M. K. Gaillard and B. W. Lee, Phys. Rev. Lett. **33**, 108 (1974); G. Altarelli and L. Maiani, Phys. Lett. B **52**, 351 (1974).

[43] M. A. Shifman, A. I. Vainshtein, and V. I. Zakharov, Nucl. Phys. **B120**, 316 (1977); Sov. Phys. JETP **45**, 670 (1977).

[44] F. J. Gilman and M. B. Wise, Phys. Rev. D **20**, 2392 (1979); **27**, 1128 (1983); B. Guberina and R. D. Peccei, Nucl. Phys. **B163**, 289 (1980).

[45] A. J. Buras, M. Jamin, M. E. Lautenbacher, and P. H. Weisz, Nucl. Phys. **B400**, 37 (1993); **B400**, 75 (1993); A. J. Buras, M. Jamin, and M. E. Lautenbacher, Nucl. Phys. **B408**, 209 (1993).

[46] M. Ciuchini, E. Franco, G. Martinelli, and L. Reina, Phys. Lett. B **301**, 263 (1993).

[47] W. A. Bardeen, A. J. Buras, and J.-M. Gérard, Phys. Lett. B **180**, 133 (1986); **192**, 138 (1987); Nucl. Phys. **B293**, 787 (1987).

[48] T. Hambye *et al.*, Phys. Rev. D **58**, 014017 (1998); T. Hambye, G. Köhler, and P. H. Soldan, Eur. Phys. J. C **10**, 271 (1999); T. Hambye *et al.*, Nucl. Phys. **B564**, 391 (2000).

[49] J. Bijnens and J. Prades, J. High Energy Phys. 01 (1999) 023; 06 (2000) 035.

[50] S. Bertolini *et al.*, Nucl. Phys. **B514**, 63 (1998).

[51] S. Peris and E. de Rafael, Phys. Lett. B **490**, 213 (2000); arXiv:hep-ph/0006146 v3.

[52] J. Bijnens and J. Prades, J. High Energy Phys. 01 (2000) 002.

[53] S. Herrlich and U. Nierste, Nucl. Phys. **B419**, 292 (1994); Phys. Rev. D **52**, 6505 (1995); Nucl. Phys. **B476**, 27 (1996).

[54] A. Pich and E. de Rafael, Phys. Lett. B **374**, 186 (1996).

[55] O. Cata and S. Peris, J. High Energy Phys. 03 (2003) 060.

[56] J. Bijnens and J. Prades, Phys. Lett. B **342**, 331 (1995); J. High Energy Phys. 01 (2000) 002; J. Bijnens, E. Gamiz, and J. Prades, J. High Energy Phys. 03 (2006) 048.

[57] W. Lee *et al.*, Phys. Rev. D **71**, 094501 (2005); Y. Aoki *et al.*, Phys. Rev. D **72**, 114505 (2005); arXiv:hep-lat/0508011; E. Gámiz, S. Collins, C. T. H. Davies, J. Shigemitsu, and W. Wingate, Proc. Sci., LAT2005 (2006) 347; T. Bae, J. Kim, and W. Lee, *ibid.*, LAT2005 (2006) 335; LAT2005 (2006) 338; S. Cohen, *ibid.*, LAT2005 (2006) 346; F. Mescia *et al.*, *ibid.*, LAT2005 (2006) 365; J. M. Flynn, F. Mescia, and A. S. B. Tariq, J. High Energy Phys. 11 (2004) 049.

[58] P. Dimopoulos *et al.*, Nucl. Phys. **B749**, 69 (2006); D. Becirevic *et al.*, Eur. Phys. J. C **37**, 315 (2004), and references therein.

[59] See e.g. J. Bijnens and J. Prades, Nucl. Phys. **B444**, 523 (1995).
[60] G. Buchalla, A. J. Buras, and M. E. Lautenbacher, Rev. Mod. Phys. **68**, 1125 (1996).
[61] D. T. Son and M. A. Stephanov, Phys. Rev. D **69**, 065020

(2004).
[62] M. A. Shifman, A. I. Vainshtein, and V. I. Zakharov, Nucl. Phys. **B147**, 385 (1979).
[63] A. Karch, E. Katz, D. T. Son, and M. A. Stephanov, Phys. Rev. D **74**, 015005 (2006).